Remote Sens. **2012**, *4*, 271-302; doi:10.3390/rs4010271

OPEN ACCESS

Remote Sensing

ISSN 2072-4292

www.mdpi.com/journal/remotesensing

Article

Environmental and Sensor Limitations in Optical Remote Sensing of Coral Reefs: Implications for Monitoring and Sensor Design

John D. Hedley [1,2,*], Chris M. Roelfsema [3], Stuart R. Phinn [3] and Peter J. Mumby [1,4]

[1] School of Biosciences, University of Exeter, Prince of Wales Road, Exeter EX4 4PS, UK

[2] ARGANS Ltd., Tamar Science Park, Derriford, Plymouth PL6 8BT, UK

[3] Center for Spatial Environmental Research, School of Geography Planning and Environmental Management, University of Queensland, Brisbane, QLD 4072, Australia; E-Mails: c.roelfsema@uq.edu.au (C.M.R.); s.phinn@uq.edu.au (S.R.P.)

[4] Marine Spatial Ecology Lab, School of Biological Sciences, University of Queensland, Brisbane, QLD 4072, Australia; E-Mail: p.j.mumby@uq.edu.au

* Author to whom correspondence should be addressed; E-Mail: jhedley@argans.co.uk; Tel.: +44-1752-764-298; Fax: +44-1752-772-227.

Received: 1 December 2011; in revised form: 9 January 2012 / Accepted: 9 January 2012 / Published: 23 January 2012

Abstract: A generic method was developed for analysing the capabilities of optical remote sensing of aquatic systems in terms of environmental components and imaging sensor configurations. The method was based on a component based model of the entire system in which not only benthic composition but other environmental components such as water inherent optical properties (IOPs), bathymetry, sun elevation, wind speed and sensor noise characteristics were defined by datasets with the potential to include across-image variation. The model was applied to data from Pacific Ocean reefs in an airborne sensor context to estimate the primary environmental or sensor factors confounding discrimination of benthic mixtures of key reef types: live coral, bleached coral, dead coral and macroalgae. Results indicate that spectral variation of benthic types and sub-pixel mixing is the primary limiting factor for benthic mapping objectives, whereas instrument noise levels are a minor factor.

Keywords: remote sensing; benthic; aquatic; inherent optical properties; coral reefs; bleaching

1. Introduction

Analysis of satellite and airborne imagery has shown that remote sensing offers the potential to monitor important ecological events on coral reefs, such as stress induced coral bleaching (loss of symbiotic zooxanthellae [1], coral mortality and phase shifts to macroalgal dominance [2,3]. However, practical image-based coral reef remote sensing research has, by necessity, been performed on a rather *ad hoc* basis, producing a variety results that are sensor-specific, algorithm-specific and site-specific [3–5]. Clearly, application-based results are an inefficient method to estimate the maximum potential of coral reef remote sensing in general terms, or to demonstrate how to realise that potential through analytical algorithms and sensor design. Modelling studies are therefore required to evaluate the upper or lower theoretical bounds of remote sensing capability and guide the design of appropriate sensors. Various studies have assessed the spectral separability of reef benthic classes and in some cases advised on optimal wavelengths for discrimination [6–10]. However, these studies have focused on variation in benthic type *in situ* spectral reflectance and sensor noise as the primary sources of noise in the system. In reality, within the spatial scale of a single remotely-sensed image, coral reef waters can exhibit a wide range of water clarity from Case 1 oceanic-like fore-reef sites through shallow lagoonal sites subject to wind and tidal driven re-suspension of sediments, to complex sediment and CDOM-loaded terrestrial inputs [11,12]. Around spur and groove zones and on patch reefs depth can also vary with vertical scales almost equal to the total height of the water column. The spectral signal for a given benthic type is therefore subject to these additional variations within an image, and discrimination may be consequently confounded. Put simply, two distinct benthic types at different depths (for example) may be spectrally indistinguishable in a remotely sensed image.

Previous studies have shown that basic reef benthic types such as coral, macroalgae, seagrass and sand are fundamentally separable by hyperspectral reflectance signatures [5,6,8,13]. Thus, modelling water column radiative transfer without factoring-in any variation in clarity or depth leads to the inevitable conclusion that, assuming optimal spectral bands, sensor signal-to-noise characteristics (SNR) are the predominant limiting factor and that remote sensing capability is "sensor limited", *i.e.*, reflectance spectra at depth are increasingly similar but still technically separable by a sensor with a high SNR (Figure 1). In reality, however, the system may be "environmentally limited" with sensor SNR issues becoming insignificant compared to the variation in reflectance caused by variance in water column depth and optical properties (Figure 1). Since these processes will also be a function of wavelength, the number, position and width of the sensor spectral bands will also contribute to "sensor limitation". Sensor spatial resolution and the spatial heterogeneity of target features will also interact to introduce sub-pixel spectral mixing and reduce the capability for benthic class discrimination. Depending on perspective, this process could be considered either a sensor limitation or an environmental limitation.

Figure 1. Sensor-limited *vs.* environmentally limited remote sensing. At each stage of the remote sensing system the variation in classes to be discriminated is expressed by the distribution of their member populations in spectral space, e.g., as illustrated in two bands b1, b2. The extent of overlap between two classes expresses their fundamental inseparability. Variation in different components of the system, such as benthic class spectral variation, variance in water clarity, or sensor noise, contributes to overall variation in the recorded signal. Sensor-limited objectives are those for which a change in sensor design characteristics will improve separability despite environmental sources of variation. A possible measure of class overlap is to attempt to insert a separating plane in spectral space between A and B, linear discriminant analysis (LDA) is one method to achieve this.

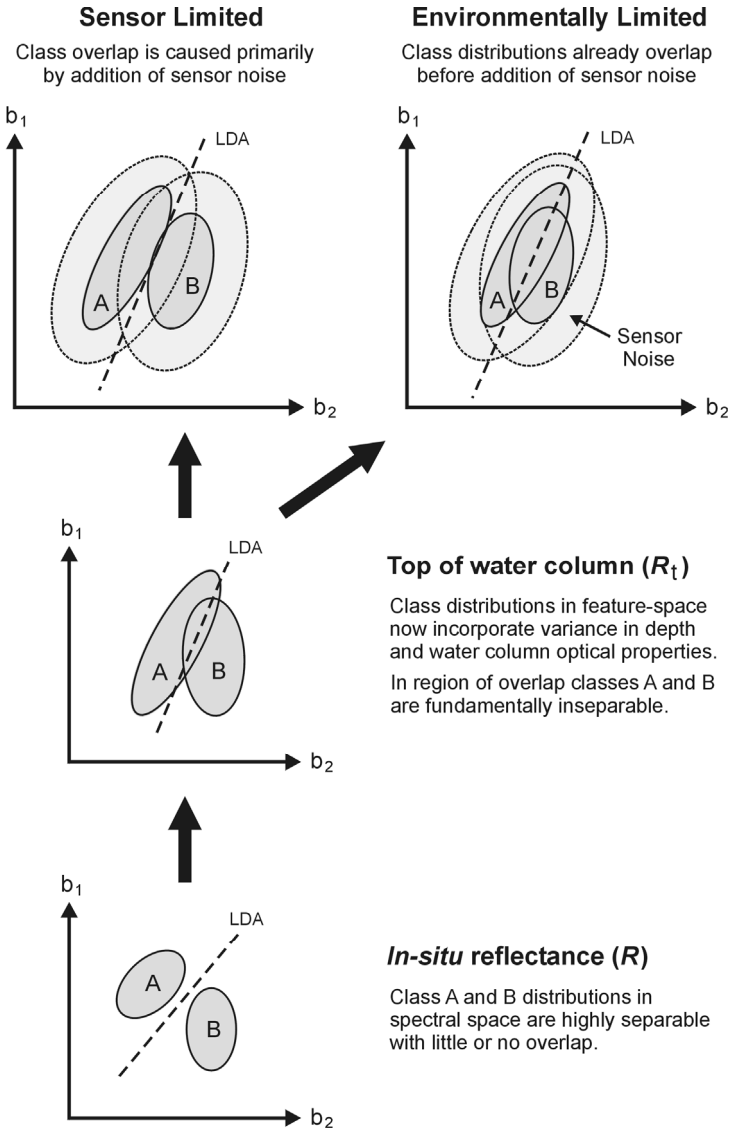

Estimating benthic class separability of *in situ* spectra or at specific depths [6,9] is of little practical relevance when in general, without ancillary data, the depth of individual pixels in a remotely sensed image is unknown. Rather, the separability of classes as they appear across the expected range of depths is more relevant (Figure 2). Put simply, there may be a problem where "coral" at one depth looks like "algae" at a different depth, for example. In such cases neither depth nor benthic class can be reliably determined from reflectance alone. An important concept developed in this study is that the

variance in spectral reflectance introduced by environmental factors and sensor characteristics is key to understanding the fundamental limits of the separability of benthic classes. For example, if a model is used to estimate the above-water reflectance resulting from two distinct *in situ* benthic reflectances, as depth in increased the modelled reflectances will become increasingly similar. However the two reflectances will continues to be numerically separable unless a factor is considered which will introduce variance into the measured signal, e.g., sensor noise, or a small random variance in one of the depths. The total achievable separability is therefore a complex result of the interaction of the absolute effect and variance induced by the environmental and sensor components in the system, framed by the structure of the question that is to be asked of the data (Figure 1).

Figure 2. Hypothetical stylised example to illustrate the need to assess separability of benthic classes across a depth range. Above water reflectance measured in two bands (b1, b2) shows the basic within-class variance in *in situ* reflectances of two benthic classes (A and B) shifted at the specific depths 1, 2 and 3 m, (**a**) and (**b**). Any pair-wise comparison between A and B at two specific depths indicates high separability ~65% (**c**). However, given that A and B can occur at any depth, for very few values of b1 and b2 can the benthic class be unequivocally identified as A or B and the actual separability of A and B is very low ~15% (**d**). Pair-wise comparisons (c) cannot be combined to reveal the overall separability (d) since there is no way to know that the individual overlap regions combine to give (d).

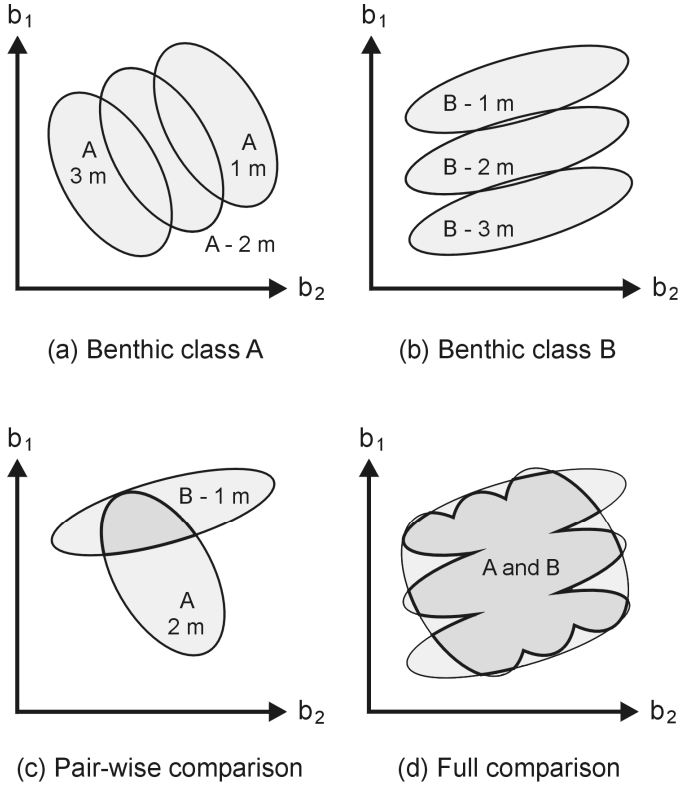

The recent trend in analysis algorithms for shallow water benthic remote sensing is to seek a pixel-by-pixel best fit for reflectance from a forward-based radiative transfer model parameterised on benthic reflectance, depth, water optical properties [12,14–21]. Such algorithms offer the promise of simultaneous derivation of depth, water optical properties and benthic class. However, clearly, within

such multi-parameter models there is the possibility for confusion, where different sets of parameters produce similar predicted reflectances. This issue is another expression of the concept of a system being "environmentally limited" (Figure 1).

Various authors have discussed the possibility of a new satellite-based remote sensing instrument designed specifically for coral reef applications [6,7,10]. While these studies have focused on determining optimal band wavelengths, further work is now needed to provide concrete design advice on issues such as the trade-off between spatial resolution, spectral resolution and SNR. To justify expenditure on a new satellite sensor considerable effort must be made to evaluate the expected efficacy of the proposed design, this requires a credible assessment of the extent to which sources of environmental variance are inherently limiting. In this paper we present a methodology designed to address this question, and as first step apply it to an airborne sensor configuration with a fixed set of spectral bands (Table 1). We consider the optimal SNR and relative spatial resolution in relation to reef heterogeneity for detection of coral bleaching, mortality and algal overgrowth of live coral on a Pacific reef. While this study concentrates on reef-scale monitoring at high spatial resolutions, the limits of discrimination established are also directly relevant to satellite sensors, and the methodology is readily extendable to include atmospheric effects and different spectral band assignments.

Table 1. Band wavelengths for modelled sensor. In each band sensitivity is considered uniform from λ_{min} to λ_{max} , consistent with Compact Airborne Spectrographic Imager (CASI) configuration where each band is composed of several wavelength-contiguous sensor elements.

Band	λ_{min} (nm)	λ_{max} (nm)	Width (nm)
1	455.2	465.5	10.3
2	474.6	483.1	8.5
3	492.1	502.5	10.4
4	511.6	520.2	8.6
5	526.6	531.4	4.8
6	549.5	555.3	5.8
7	560.7	566.5	5.8
8	571.9	577.7	5.8
9	592.2	597.1	4.9
10	611.4	617.2	5.8
11	622.3	627.2	4.9
12	671.5	676.4	4.9
13	688.5	693.4	4.9
14	705.1	709.0	3.9
15	773.5	781.3	7.8

2. Methods

2.1. Overview

Our analysis considers the extent to which airborne coral reef remote sensing may be environmentally limited by spatial variation in water column properties and depth, operating in

conjunction with other environmental factors such as sub-pixel mixing from benthic classes of mixed composition, *i.e.*, spatial resolution *vs.* heterogeneity, sea surface state and sun elevation (Figure 3(b)). A modelling and sensitivity analysis was performed in which the spectral separability of benthic classes was assessed under a set of scenarios each representing a different combination of environmental factors and sensor characteristics. By comparing achievable separability under different scenarios the effects of individual environmental factors were assessed, such as the difference between separability at specific depths as opposed to separability when the benthic classes occur across a range of depths. Previous work has considered sensor spectral band configurations for coral reef applications [6,7]. For statistical validity, given the large number of degrees of freedom in configuring a hyperspectral sensor, this requires a very substantial dataset of reflectances (*i.e.*, 1,000's). So to simplify the analysis here, we used a single configuration of sensor wavelength bands throughout (Table 1) and concentrate on sensor noise and sub-pixel mixing, the latter being analogous to the effect of spatial resolution. The band choices are based on a review of coral and algal pigment absorption features from spectroscopy and remote sensing [4], and actual configurations of the Compact Airborne Spectrographic Imager (CASI) used in previous studies which have demonstrated discrimination of live and dead coral [2,3]. The structure of the methods and analysis are summarised in the flowchart of Figure 3(a), and the details are presented in the following sections.

2.2. Sensitivity Analysis Structure

The sensitivity analysis involved modelling the distribution of sensor recorded spectral reflectance for each benthic class under specific scenarios defined by the other environmental and sensor factors. Note we use the term "scenario" to represent a particular combination of environmental factors and sensor configuration (Figure 3(b), Table 2). The separability of the reflectance distributions for differing benthic compositions (Figure 1) under a given class combination scenario indicates the extent to which that particular combination of environmental factors and sensor configuration confounded separability for those benthic classes.

In the benthic remote sensing literature the concept of "class" is often restricted to benthos, since "classification" of image pixels to benthic classes is usually the final aim [22]. However, as Mobley [23] discusses, the translation of class structured analyses as used in terrestrial applications to sub-surface aquatic environments is problematic, since benthic composition is only one of several environmental and sensor factors that contribute to the sensor recorded signal. In our analysis we conceive a class structure for the other environmental factors and sensor configurations (Table 2). For example, in the same way that the pure Live Coral benthic class was modelled as a set of reflectance spectra from live corals, the Zonal IOP class was modelled as a set of water optical properties collected across different reef zone locations. This is conceptually similar to the structure of image analysis methods which use look up tables or model inversions based on a range of water optical properties [16,18] but here some classes are explicitly constructed to encompass within-class variance of the parameters in question. By this method, parameters often treated as quantitative, such as depth [16] can be class structured by quantizing the value range in a manner suitable for the application and then grouping discrete values into classes (Table 2).

Figure 3. Methods flowchart (**a**) and sensitivity analysis structure (**b**). Each combination of benthic type, environmental component and sensor SNR treatment corresponds to a single model scenario. For each scenario the representative distribution of total remote sensing reflectance, R_t, is estimated by radiative transfer modelling. The separabilities between scenarios with differing benthic types and identical environmental and sensor treatments are estimated in spectral space. The hierarchical analysis reveals which sensor and environmental treatments have the greatest effect in reducing benthic type separability.

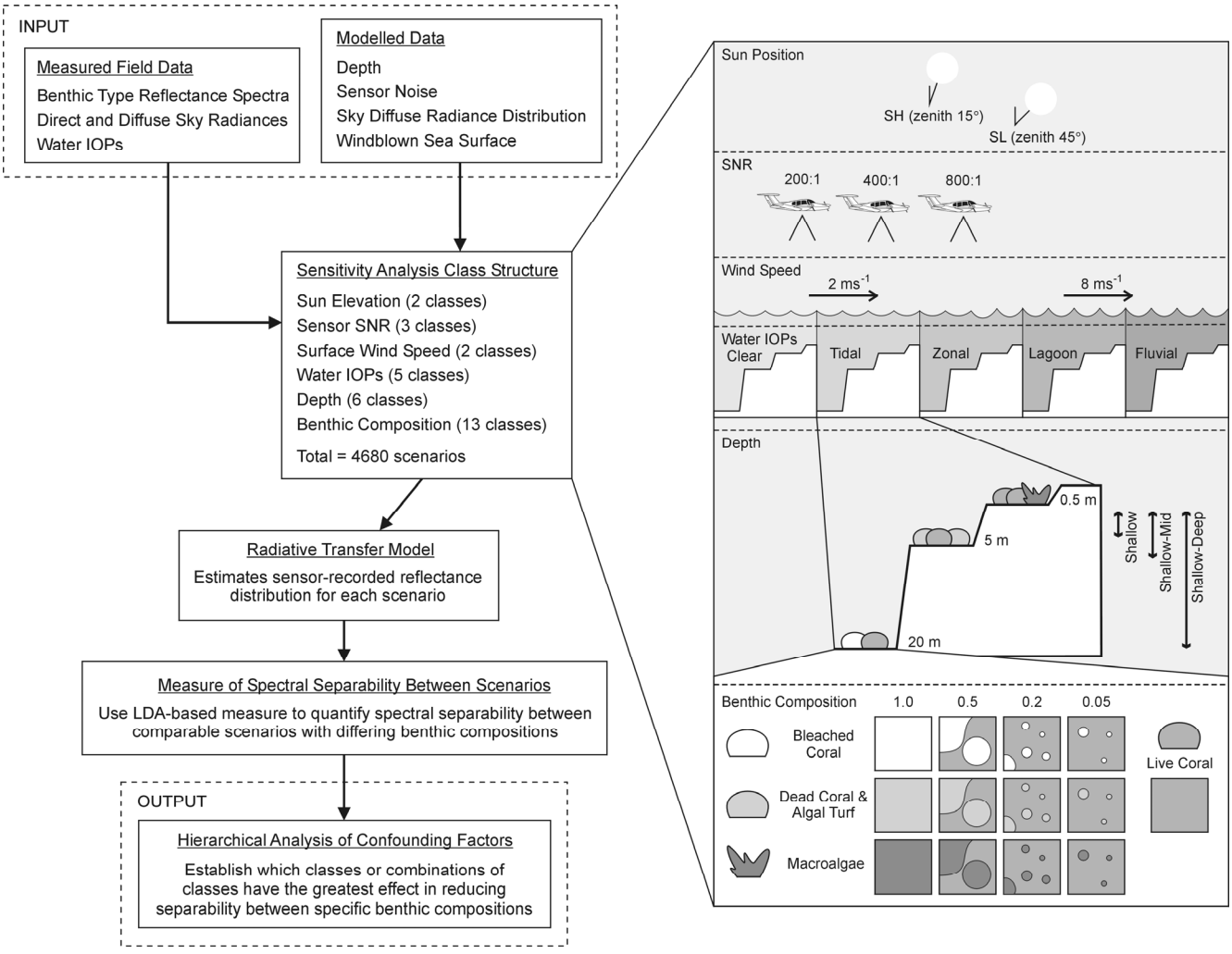

(**a**) (**b**)

The class structure of the sensitivity analysis included thirteen benthic classes (based on linear spectral mixes of four basic benthic types, each represented by a number of spectra, Table 3), five water inherent optical property (IOP) classes, six depth classes, two sun position classes, two wind speed classes and three sensor SNR classes (Table 2, Figure 2(b)). A "scenario" therefore refers to modelling of sensor recorded reflectance distribution under a specific combination of the environmental and sensor classes. The overall structure of the results was therefore 6-dimensional, with every possible combination of the different classes evaluated giving 4,680 scenarios (Figure 2(a)). The reflectance distributions for each of these scenarios were then compared to assess the spectral separability of the scenarios based on 100% Live Coral cover from the corresponding scenarios for the other twelve benthic classes (corresponding scenarios have all other environmental and sensor classes

the same). This gave a total of 4,320 individual separability evaluations: three groups of 1,440 scenarios corresponding to discrimination of pure Live Coral from mixtures containing Bleached Coral, Dead Coral/Turf and Macroalgae respectively. For each of these three benthic class groups a hierarchical master analysis (described below) organised the 1,440 results into a graph diagram structure revealing the most significant environmental and sensor classes with respect to reducing the separability of the benthic compositions from pure Live Coral.

Table 2. Structure of the multi-factor sensitivity analysis. Emboldened classes have within-class variance, non-emboldened represent factors uniform across an image.

Component and Classes	Description
Benthic Composition Reflectance Distribution (13 Classes)	
Live Coral 100% cover **Bleached Coral in Live Coral** (proportion 1.0, 0.5, 0.2, 0.05) **Dead Coral in Live Coral** (proportion 1.0, 0.5, 0.2, 0.05) **Macroalgae in Live Coral** (proportion 1.0, 0.5, 0.2, 0.05)	Each class is represented by 200 randomly generated diffuse spectral reflectance profiles constructed as a proportional linear mix between two random *in situ* reflectance spectra drawn from the field collected spectral library (Table 3, Figure 4). Linear spectral mixing at the bottom of the water column was therefore assumed [24]. The figure of 200 spectra per class was determined experimentally to ensure the variation in the *in situ* libraries was fully exploited while, for computational efficiency, excessive numbers of spectra were not propagated through the model (see Results and Discussion.
Depth (6 Classes)	
0.5 m, 5 m, 20 m	Three image-uniform classes representing specific absolute depths of 0.5 m, 5 m and 20 m respectively.
Shallow (0.5–2 m) **Shallow-Mid (0.5–5 m)** **Shallow-Deep (0.5–20 m)**	Three image-variable classes each of which models a remotely sensed image in which variation in depth is present. Shallow contains the two depths 0.5 m, 2 m; Shallow-Mid contains, 0.5 m, 2 m and 5 m; Shallow-Deep contains those three plus 10 m and 20 m. For example, the structure of the Shallow-Deep class implies that one of every five image pixels on the reef would be at 20 m.
IOPs (5 Classes)	
Clear	An image-uniform class represented by a single IOP dataset from a fore reef drop-off site with strong tidal flushing (Figure 5)
Lagoon	An image-uniform class represented by a single IOP dataset from a lagoonal station (Figure 5).
Tidal	Image-variable class containing four datasets from a fore-reef location collected at two-hour intervals in a tidal cycle (Figure 5).
Zonal	Image-variable class containing five IOP datasets from a mixture of lagoonal and fore-reef sites (Figure 5).
Fluvial	Image-variable class with the same IOP datasets as Zonal plus two acquired at 0.6 km and 1 km offshore from a river outfall that passes through dense mangroves (Figure 5).
Sun Elevation (2 Classes)	
SH (zenith angle 15°) SL (zenith angle 45°)	Two image-uniform sky radiance distributions based on field data acquisitions of total and diffuse shaded downwelling irradiance collected in the marine tropics at two sun elevations. The directional sky radiance distribution was modelled as the sum of the direct sun radiance (total minus diffuse) and the diffuse irradiance directionally weighted by a clear sky radiance model [25].
Wind Speed (2 Classes)	
W2 (2 ms^{-1}) W8 (8 ms^{-1})	Two image-uniform water surface classes based on the approximate minimum and maximum daily wind speed averages taken over a one month period in Palau, April 2006 (this month coincides with a field study not reported here). These wind speeds are also similar to the range cited in previous remote sensing field studies, e.g., 2 ms^{-1} [9], ~5 ms^{-1}, [12]. The sea surface state is incorporated into the radiative transfer model by a statistical derivation of the directional light reflection and transfer with a relative sun and wind azimuth angle of 45°, modelled according to Cox and Munk wave slope statistics [26,27].
Sensor SNR (3 Classes)	
200:1 **400:1** **800:1**	Three SNR values defined as the ratio of the standard deviation of a normally distributed noise term to the signal level in each band [28]. Values were chosen to be representative of those cited for existing airborne remote sensing instruments (e.g., 480:1 and peak 790:1 for CASI and CASI-2, and 500:1 to 1000:1 for HyMap [29], www.itres.com). SNR classes implicitly embody within-image variance as they are a source of spectral variation on a pixel-by-pixel basis.

Table 3. Genera breakdown of reflectance spectra samples for the four basic benthic types. In situ reflectance Data were collected in 2006 at various times and locations in Fiji (South Pacific), Palau (Micronesia) and Heron and Keppel Islands (Great Barrier Reef). The majority of the bleached coral spectra samples were collected during a single bleaching event at Keppel Islands March 2006.

Category	Total Spectra	Genera	Number of Spectra
Live Coral	233	*Acropora*	87
		Porites	45
		Montipora	17
		Pocillopora	12
		Favites	7
		Millepora	6
		Others (< 5 each)	59
Bleached Coral	37	*Acropora*	32
		Others	5
Dead Coral/Turf Algae	66	N/A	
Macroalgae	97	*Halimeda*	12
		Lobophora	11
		Padina	10
		Sargassum	9
		Laurencia	8
		Chlorodesmus	7
		Dictyota	6
		Caulerpa	5
		Others (<5 each)	29

2.3. Radiative Transfer Model

The benthic classes were each initially represented by a set of *in situ* recorded spectral reflectances linearly mixed according to the benthic composition (Table 3, Figure 4, collection methods given in [24]). In the analysis these basic reflectance spectra were translated by modelling to give total spectral reflectance above the water surface, R_t, based on the parameters defined by a given set of the other system component classes and incorporating sensor noise. For example, an initial set of 200 *in situ* reflectance spectra of benthic class for pure Live Coral could, in one scenario, be modelled to give 200 above-surface reflectance spectra under clear water conditions, 5 m depth, wind speed of 2 ms^{-1} and sun zenith angle of 15°. However, like the benthic classes, some environmental component classes were also based on multiple data to express their within-class variance. For example, the Zonal IOP class (Table 2) consisted of five different IOP datasets from different reef locations; in this case the modelling process would result in 1,000 R_t spectra, the distribution of which embodies both variance in benthic reflectance and water optical properties. By assessing the spectral separability of two benthic classes based on their modelled R_t spectra under a given combination of system components the impact of the additional sources of variance was assessed.

Figure 4. Benthic type *in situ* reflectances. For each type 15 spectral reflectances drawn at random from the full spectral library are shown.

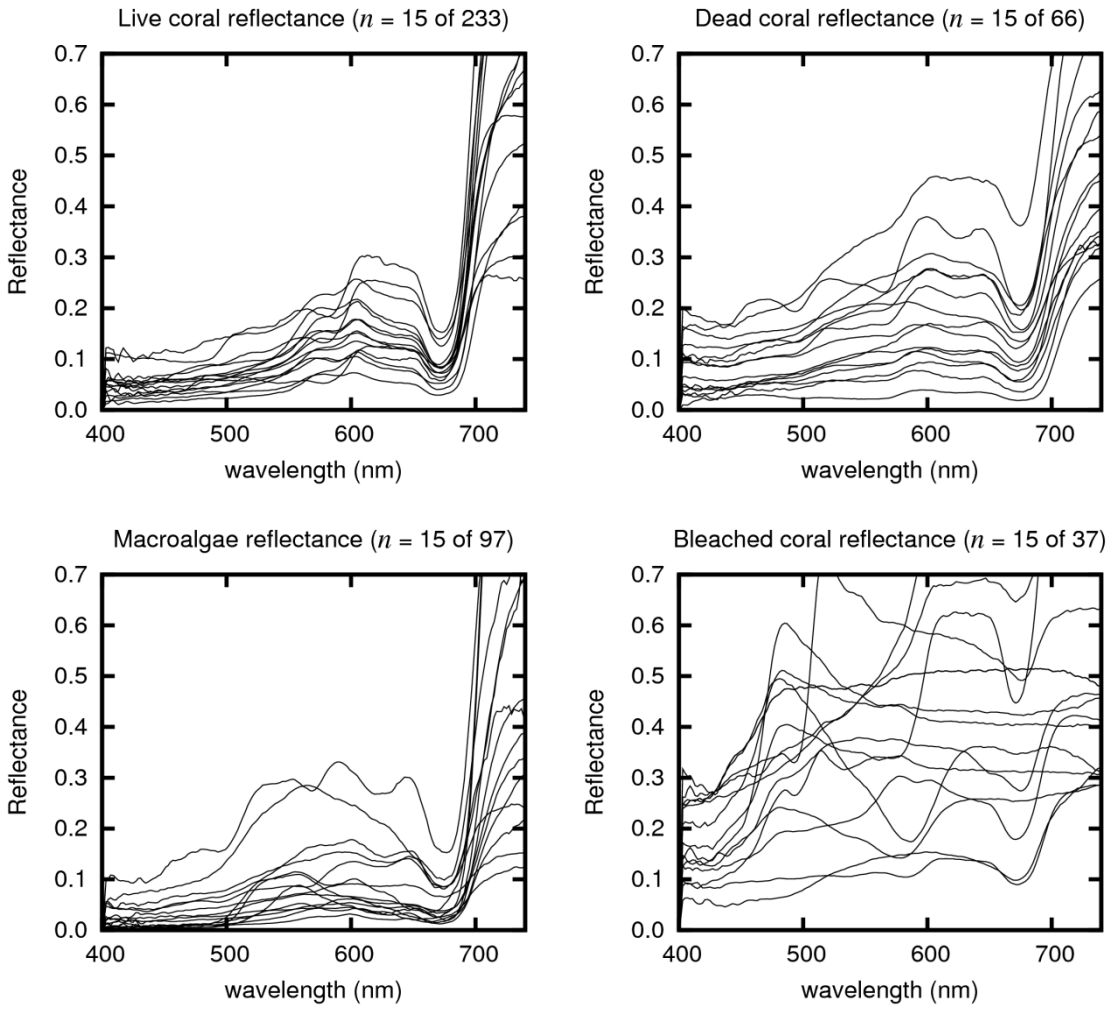

The technical steps in the modelling process were as follows. The benthic class reflectance spectra, IOPs and input sky irradiances (Table 2) were resampled to a typical 15-band CASI sensor configuration (Table 1) prior to the modelling phase. The modelling of R_t from benthic reflectance was performed using PlanarRad, an open-source implementation of the invariant imbedded algorithm for directional "quad-averaged" radiances in plane-parallel waters. This software is functionally equivalent to the commercial software Hydrolight and has been validated against both Hydrolight and other models [31,32] (and unpublished data). Total above-water reflectance was calculated as $R_t = L_u/E_d$, where L_u is the upwelling radiance and E_d is downwelling irradiance just above the water surface. We use R_t since unlike the usual definition of remote sensing reflectance, R_{rs}, [27] our use of L_u (and hence R_t) includes reflection from the water surface. This may be an important confounding factor for benthic separability since a high sun-glint signal increases magnitude of SNR-based sensor noise, which being stochastic cannot be corrected for even if the sun-glint component itself can be removed [33]. Sensor noise was incorporated onto the R_t spectra produced by the water column model by translating each R_t into 30 new spectra each of which had random noise terms added in each band based on the sensor SNR class for that scenario (Table 2). The figure of 30 was chosen heuristically prior to the main

analysis with the objective being to fully populate the signal noise in the 15-band spectral space without excessive redundancy.

Figure 5. Optical properties of IOP datasets used in the IOP class definitions. (**Left**): total spectral beam attenuation of Tidal class comprising four datasets sampled at approximately 2 h intervals showing tidal variation on a fore-reef site. (**Centre**): Clear and Lagoon classes are each represented by single dataset. The Zonal class contains both Clear and Lagoon datasets and three others from lagoonal and fore-reef locations. The Fluvial class contains all the datasets of the Zonal class plus two others taken in proximity to a river outflow. (**Right**): modelled diffuse attenuation k_d (solar zenith angle 15°, over 5 m depth with live coral substrate) of the clearest and most turbid IOP datasets compared to Jerlov water types I, IA, IB, II, III and 1 (from bottom to top [27]).

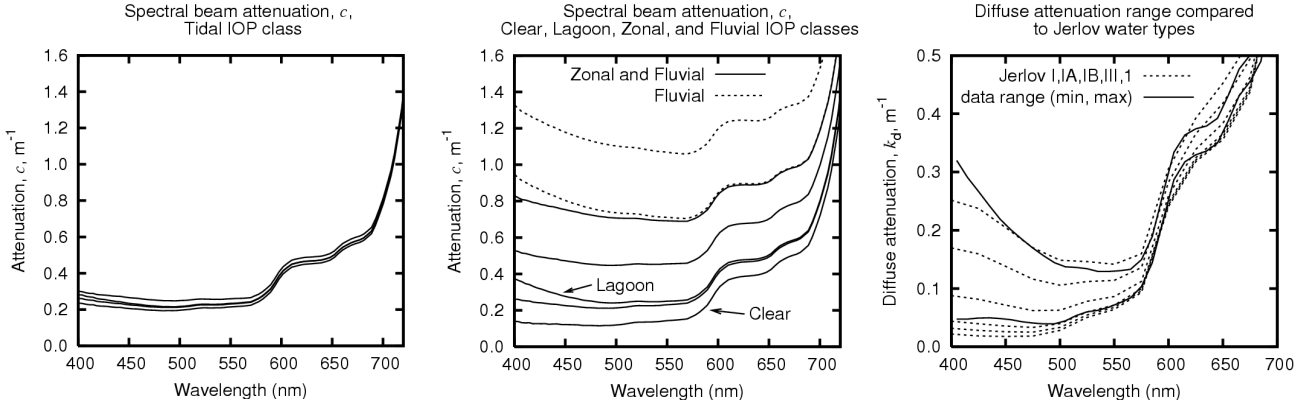

The water column model requires depth-averaged water inherent optical properties as input (Table 2, Figure 5). These data were collected at various reef locations in Palau, Micronesia, in March 2006 using a WET Labs AC-S, measuring the non-pure water fraction beam attenuation and absorption in 85 bands from 400 nm to 740 nm, and a WET Labs ECO-BB3 backscatter meter, measuring backscatter at 117° at 470 nm, 532 nm, and 660 nm. The AC-S data were subject to full temperature, salinity and scattering corrections as described in the WET Labs protocol document and [34]. The resulting non-pure water fraction absorption (typically denoted *a*) and attenuation (*c*) were added back onto pure water values [35] to give the total *a*, *b* (scattering) and *c* values for modelling purposes (Figure 5). The backscatter at 117° was processed to estimate total particulate backscatter B_p as described in [36], and this formed the basis for the estimation of three Fournier-Forand phase functions, at 470 nm, 532 nm, and 660 nm, according the methods described in [37] with functions for other wavelengths derived by linear interpolation. With respect to modelled diffuse attenuation for sun zenith 15°, the range in the IOP data set is greater than that of Jerlov types IB to 1 (Figure 5) but slightly less than that of a previously published Caribbean diffuse attenuation dataset [38].

2.4. Measure of Spectral Separability between Scenarios

To assess spectral separability between scenarios it was desired to find a measure which approximates to the intuitive notion of class overlap in spectral space (Figure 1). The method used here was to attempt to insert a separating plane in spectral space between the modelled reflectances of the

two benthic types (Figure 1). The inverse of the grouped covariance matrix is one way to establish such a plane and is similar to linear discriminant analysis (LDA) [39]. For each pair of benthic classes and a specific set of treatments (a scenario) the set of n R_t spectra representing each class was used to establish a dividing plane in spectral space (Figure 1) and the number of individual spectra lying on their correct class side of the plane was counted as n_c. Note that n_c ranges from n to $2n$ since there are a total of $2n$ spectra and a separating plane can always be found such that half the points are on the correct class side (Figure 1). Separability, τ, was then calculated as,

$$\tau = 100 \times \frac{n_c - n}{n} \ (\%) \tag{1}$$

In practice, the range of τ is 0% (completely inseparable classes) to 100% (completely separable) and has identical interpretation to the Tau coefficient [40] as the percentage more correct classifications achieved than would be expected by chance alone [22]. An individual τ value has no associated statistical significance and is simply a number that approximates to the fundamental separability between the spectral distributions for a specific model evaluation (Figure 1).

The fully factored sensitivity analysis contained 4,680 class combinations (*i.e.*, scenarios) that corresponded to modelling approximately 1,560,000 R_t spectra, before the addition of sensor noise. For each comparison between scenarios the τ value gives the resultant separability for that particular model evaluation with no associated statistical significance. However, since some classes contained stochastic elements, e.g., benthic class mixtures and sensor noise, the predicted separabilities are estimates of what would be expected under many model runs for the given scenarios. To assess the spread of these estimates the entire analysis was repeated ten times. In the results the mean separabilities ($\bar{\tau}$) are reported with reference to their standard error over the ten runs. Where required, *t*-tests were applied to these mean separabilities to determine if an apparent change in separability were genuine or an artefact of the specific instantiations of stochastic components of the model. Where this was done simultaneously across several scenarios both the standard and Dunn-Ŝidák Type I error corrected results were calculated [41].

2.5. Hierarchical Analysis of Confounding Factors

With 4,680 class combinations in a 6-dimensional results table further condensing of the results is required to get an overview of relative importance of the different factors. Here we present a general method of constructing a hierarchical class significance diagram from a fully factorised sensitivity analysis (Figure 6).

The diagram consists of a directed graph (meaning "graph" as in graph theory [42]) that is built starting with a single vertex representing the entire results, *i.e.*, all scenarios, and then scenarios including specific classes are iteratively excluded with the classes chosen in order to maximally increase the overall accuracy at each step. The result is a directed graph where each arc represents the exclusion of a class from the entire results table and vertices represent the resulting subsets of scenarios. The vertical position of a vertex in the diagram is based on the mean separability over the set of scenarios that it represents. Therefore the relative effect of excluding successive confounding classes is readily apparent. The horizontal position of vertices has no meaning and is merely based on spacing out the vertices at each level. The graph is built iteratively, for each current vertex each class is

removed in turn and the increase in overall accuracy noted. Then new vertices and arcs are added corresponding to the class giving the highest increase in overall accuracy when excluded, and any other classes which have an effect on overall accuracy of at least half as much as the highest. More than one class may be added at each step since, for example, excluding the depth class of 20 m from the results might cause a similar increase in overall accuracy to removing the Zonal IOP class. In addition, different "routes" from low to high accuracy may merge to give collections of classes that jointly act to confound accuracy. Figure 6 illustrates the construction of a hierarchical class significance diagram from a simple hypothetical three-factor sensitivity analysis.

Figure 6. Example construction of an hierarchical analysis diagram. Eight scenarios are produced from a three-factor analysis as all combinations of A1,A2; B1,B2; and C1,C2. The mean separability over all scenarios is 54%, represented by the vertical position of the "All Classes" node. The horizontal position of nodes has no meaning. The left edge of the diagram represents the exclusion of classes B1, A2 and C2 (successive right hand columns of the table). Factors at the lower part of the diagram have the least effect on separability.

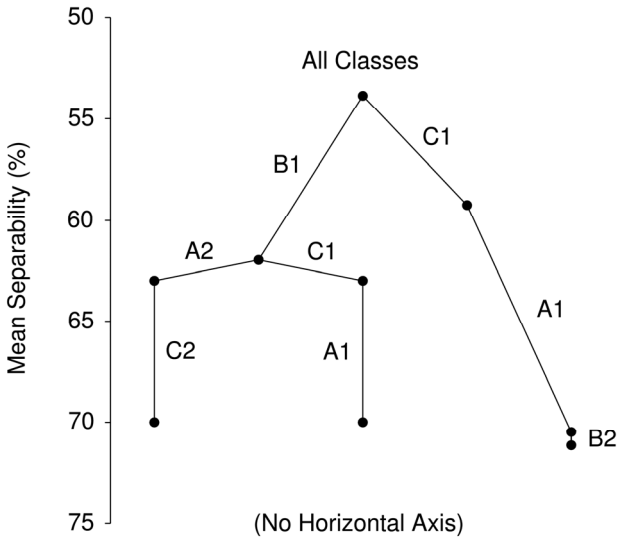

			Separabilities (%)			
				Example Exclusions		
Scenarios			-	B1	B1,A2	B1,A2,C2
A1	B1	C1	52			
A1	B1	C2	40			
A1	B2	C1	70	70	70	70
A1	B2	C2	56	56	56	
A2	B1	C1	20			
A2	B1	C2	72			
A2	B2	C1	52	52		
A2	B2	C2	70	70		
		Mean:	**54**	**62**	**63**	**70**

3. Results and Discussion

In this section, the results from the basic *in situ* separability of benthic classes in the absence of a water column are briefly considered followed by a detailed discussion of the sensitivity analysis results for each modelled environmental and sensor factor in turn. We then present the hierarchical master analysis that distils the entire sensitivity analysis into a single diagram for each benthic class group, illustrating the relative importance of environmental and sensor factors in limiting achievable discrimination accuracy in each case.

3.1. In situ *Spectral Separabilities of Benthic Classes*

The baseline *in situ* spectral separability of Bleached Coral, Dead Coral and Macroalgae from Live Coral both as pure class spectra and as mixtures in pure Live Coral was generally high (Figure 7). All three types were highly separable from Live Coral in 100% proportions, for class sizes of $n \geq 200$,

Dead Coral and Macroalgae had separabilities $\tau > 90\%$ and Bleached Coral $\tau > 80\%$. This result agrees with previously published results that fundamental reef benthic classes are highly separable by their basic *in situ* reflectance spectra [6]. However, separability between pure Live Coral and Live Coral mixed with small proportions of the other benthic types was significantly lower, dropping to $\tau < 30\%$ for mixtures of proportion 0.05. Previously published work [7] has shown that classification of linearly mixed in situ spectra of coral, algae and sand generally classifies to the dominant benthic type. Our results do not contradict this, but additionally indicate that non-dominant proportions do retain some statistical separability, at least to sub-pixel proportions of 0.2. However, in practical terms separabilities less than 50% accuracy should be considered quite weak.

Figure 7. Separabilities of *in situ* reflectance spectra and determination of optimal size (n) of mixture sets for modelling. Benthic classes are mixtures of Live Coral with Bleached Coral, Dead Coral and Macroalgae in proportions (p) of 1.0, 0.5, 0.2 and 0.05, $p = 1.0$ corresponds to pure benthic type with no Live Coral. For each class, separability is assessed against pure Live Coral based on n randomly generated linear spectral mixtures from the library spectra. For $n > 200$ horizontal lines indicate the statistical variation of the library is fully exploited. Error bars: ±1 S.D. over 100 repeats.

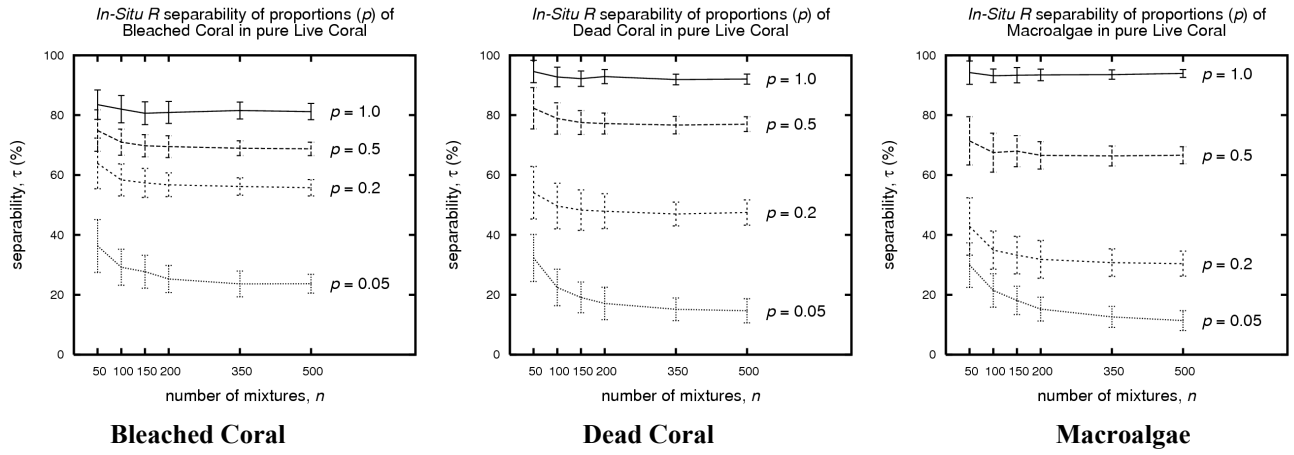

The estimated separability of pure Bleached Coral from pure Live Coral was the lowest of the three pure classes, $\tau = 81\%$ separable *vs.* 92% and 93%, $n = 200$. However, Bleached Coral separability was more robust in small proportions than for the other benthic types, with a 0.2 proportion of Bleached Coral giving $\tau = 57\%$ separability *vs.* 48% for Dead Coral and 32% for Macroalgae (Figure 7). This pattern may have two explanations: (i) an artefact due to the relatively low number of bleached spectra in the spectral library, or (ii) due to a bimodal or otherwise non-uniform relative spectral distribution of the Live Coral and Bleached Coral types, if there were two "types" of Bleached Coral, for example. The bleached coral spectral library has a far greater diversity of spectral shapes than the other benthic types (Figure 4). There is a wide range of overall reflectance, some spectra contain host pigment fluorescence features [4] in the region 450–650 nm and chlorophyll features often persist from remaining symbionts or endolithic algae [4]. Almost all the bleached spectra were collected at a single site (Keppel Islands, Australia) but the spectral diversity is higher than previously published partially bleached coral spectra [43]. However the impact of this diversity on overall separability is nevertheless

small since $\tau = 81\%$ still predicts pure Bleached Coral and Live Coral to be highly separable.

Table 4. Summary of the effect on separability of the individual sensitivity analysis factors.

Sun Elevation and Wind Speed
• At specific uniform depths, benthic class separabilities of Live Coral *vs.* Dead Coral and Macroalgae were significantly affected by sun elevation, especially for depths greater than 5 m (Figure 8). • Under any IOP class, including those with IOP variance, benthic class separabilities were significantly higher for low sun elevations (45° zenith angle *vs.* 15°). • For wind speed 2 ms^{-1} and depth ≥5 m, 239 of the 240 Live Coral *vs.* Dead Coral or Macroalgae scenarios have significantly improved separability with low sun elevation ($p < 0.05$, 168 of 240 if Dunn-Ŝidák corrected). • For wind speed 8 ms^{-1} and depth ≥5 m, 225 of the 240 Live Coral *vs.* Dead Coral or Macroalgae scenarios have significantly improved separability with low sun elevation ($p < 0.05$, 153 of 240 if Dunn-Ŝidák corrected). • Effect of sun elevation is less often statistically significant under a wind speed of 8 ms^{-1} or under Dunn-Ŝidák correction due to the overall poor separability of 0.05 proportions of Dead Coral or Macroalgae. • Overall, separability is significantly enhanced with the lower sun elevation.
Sensor SNR
• SNR was more limiting for high sun elevation, especially in the absence of depth variation. • For example, at low sun elevation separability of Live Coral and Dead Coral at 5 m was unaffected by SNR, but at high sun elevation was significantly lower for SNR 400:1 *vs.* 800:1 (Figure 8, $p < 0.0001$ for any IOP class). • Overall, for all benthic classes the difference in separability due to sun elevation was greater than that caused by doubling of sensor SNR from 400:1 to 800:1. • The limiting effect of SNR was swamped by the effect of depth variation but for SNR 200:1 was still evident (results not shown). So the interaction of sun position and SNR was still a confounding factor even under variation in depth from 0.5 m–20 m (Shallow-Deep depth class, Figure 9).
Variation in Depth and Absolute Depth
• Within-image variation in depth dampened the effect of other environmental and sensor factors such as IOP class, sun elevation or sensor SNR on benthic class separability (Figure 9 *vs.* Figure 8). • Under depth variation in all scenarios involving discriminating Bleached Coral from Live Coral, neither sensor SNR nor sun elevation had any significant effect on benthic class separability (Figure 8). • For discrimination of Dead Coral or Macroalgae from Live Coral, only a combination of low SNR (400:1) and high sun elevation produced any appreciable difference in benthic class separability.
Variation in IOP Values and Absolute IOP Value
• In shallow waters (0.5 m) neither the relative absolute clarity of the water, represented by single-dataset IOP classes or spatial variation in clarity embodied by the multiple-dataset IOP classes had much effect on the benthic class separabilities which remained at their high *in situ* levels (Figure 8). • Absolute clarity also had little effect on separability with 5 m depth, but did become important at 20 m (Figure 8). • Within-image variance in IOPs at Tidal variation levels had almost no effect, but at specific depths below 0.5 m there was some decrease in benthic class separability for Zonal and Fluvial variation (Figure 8). • Overall, absolute water clarity and Tidal or Zonal IOP variation in the absence of terrestrial inputs and at moderate depths (≤5 m) seems not to be a major confounding factor for benthic class separability. • Benthic class separabilities were often lower under the single-dataset Lagoon class than under Tidal IOP variation. Therefore, the lack of absolute clarity in the Lagoon class water (Figure 5) appeared to be more of a limiting factor than the variation in the fore-reef data due to tidal movements.

3.2. Individual Effect of Environmental and Sensor Factors

Estimated benthic class separabilities across the sensitivity analysis are the result of the interaction of all the modelled factors of benthic composition, sun elevation, wind speed, absolute depth, depth variation, absolute water clarity and variation in water clarity (Figures 8 and 9). Although strictly speaking each factor cannot be treated in isolation, some generalisations can be made. Basic trends and interesting observations are summarised in Table 4 and will be discussed briefly in this section.

In general, separability was significantly enhanced at the lower sun position zenith angle of 45° *vs.* 15° but variation in depth or low cover proportions are more severely limiting and reduced the beneficial effect (Table 4, Figures 8 and 9). Nevertheless *t*-tests indicated that the majority of Live Coral *vs.* Dead Coral or Macroalgae scenarios have significantly improved separability with low sun elevation (Table 4).

The physical basis of the advantage of low sun elevation is in reduced reflection from the air-water interface into upward radiance, L_u. For high sun elevations the benthic component is a smaller fraction of the overall larger upwelling radiance and so is increasingly obscured by sensor signal-dependent noise (SNR). This is supported by the results, however while for specific depths SNR was more limiting at high sun elevation, the effect of sun elevation itself is a greater (Figure 8). Further, when the distribution of modelled spectral reflectances (R_t) included within-image depth variation (Figure 9) the difference in separability due to sun elevation seen at specific depths (Figure 8) was almost completely absent although some SNR limitation at 400:1 and 200:1 (not shown) is still evident. These results are consistent with those presented in [9] for a simple scenario based on a HyMap image and Case 1 waters. In that study the combined sensor and environmental noise, SNR_E, in a HyMap image differed from 100:1 to 20:1 in the presence of sun glint, and consequently the calculation of theoretical depth at which live coral *vs.* dead coral can be discriminated in the clearest Case 1 reef waters is 25 m *vs.* 8 m, respectively. This result is comparable to a single class combination in our analysis, for the Clear IOP class, separability of Live Coral and Dead Coral at specific depth 5 m under high sun position (86%) is the same as at specific depth 20 m for low sun position (87%) but substantially lower with high sun position at 20 m (56%) (Figure 8, wind speed 2 ms^{-1}, SNR 800:1). However the cited study [9] did not consider the contribution to environmental noise (SNR_E) of spatial variance in IOPs or depth and also did not assess the possibility of across-depth confusion between benthic classes. These factors are incorporated into our analysis by the other treatment combinations (Table 4), and show that this specific-depth clear water result is a best case scenario for live and dead coral discrimination.

3.3. Effect of Variation in Depth vs. *Absolute Depth*

In a practical remote sensing application, the spectral distribution of above-water reflectances for a given benthic class will be subject to variance caused by differences in depth. If the depth at given pixel is unknown, the spectral reflectance could represent any benthic class at any depth within the image depth range (Figure 2). In the sensitivity analysis this corresponds to the situation where the sets of R_t representing benthic classes are modelled under a scenario involving one of the multiple-depth classes Shallow, Shallow-Mid or Shallow-Deep (Table 2). Spectral variation caused by depth variation is in itself likely to decrease the separability of the benthic classes (Figure 1). In contrast, the limiting

role of absolute depth, assessed as benthic class separability at a specific uniform depth, occurs only in conjunction with other sources of variance. For example in deep water, differences in spectral reflectance may be lower than sensor SNR thresholds, so the variance due to SNR is the fundamental cause of the inseparability. The effect of depth on separability therefore operates by two distinct mechanisms and variance in depth may in itself be limiting by increasing across-depth confusion between classes irrespective of sensor SNR (Figure 1). This reasoning is supported by the results, where the effect of variance in depth in general overwhelms the effects due to IOP class, sun elevation or sensor SNR (Table 4, Figure 9). In particular, the strong effect of sensor SNR seen at specific absolute depths below 5 m (Figure 8) is largely absent under depth variation (Figure 9), so attainable accuracy is no longer "sensor limited" but is "environmentally limited" (upper right hand part of Figure 1).

Although variation in depth reduced the significance of other factors such as sensor SNR on benthic class separability, determining the overall effect of depth variance itself, as an isolated concept, on achievable accuracy is less straightforward. From Figures 8 and 9 it appears as though overall separability under the multiple-depth classes might simply be the average separability under the specific depths within those classes. For example, if $\bar{\tau}_{S-DEEP}$ is separability under the Shallow-Deep multiple-depth class and $\bar{\tau}_d$ is separability at specific depth d m, then maybe $\bar{\tau}_{S-DEEP} \approx (\bar{\tau}_{0.5} + \bar{\tau}_2 + \bar{\tau}_5 + \bar{\tau}_{10} + \bar{\tau}_{20})/5$, since the Shallow-Deep class is constructed from the five specific depths 0.5, 2, 5, 10 and 20 m (Table 2). If the above relation were true then there would be no evidence for across-depth confusion between benthic classes and the effect of variation in depth could simply be interpreted in terms of the separabilities at the specific absolute depths involved. In fact, with respect to discriminating Live Coral from any of the other classes in pure 1.0 proportion, in 294 of 360 cases across the entire analysis the separability estimate under a multiple-depth class was significantly worse than the mean separability of the corresponding individual depths ($p < 0.01$, Dunn-Ŝidák correction applied). Separability results for many of the benthic classes with mixture proportions less than 1.0 were similarly conclusive, with the pattern only breaking down for low mixture proportions of 0.2 and 0.05, which have very low separabilities anyway.

One caveat to be considered is that the decrease in separability observed under depth variation may be an artefact of the linear separating plane (Figure 1) if depth variation produced a curved pattern of reflectance distribution in spectral space. In this case less constrained analysis methods such as successive approximation or lookup tables [17,18,20] or by applying a linearising pre-classification transform [44]. However, although the non-linear distribution argument will have some validity in general, it is an unlikely explanation of the observed results in this case for two reasons: (i) the Shallow multiple-depth class only contains two depths so depth variation alone cannot cause a non-linear distribution of R_t; and (ii) variation in IOPs would be expected to produce a similar non-linear effect in spectral distributions, but in fact in this study variation in IOPs had relatively less effect on separability than variation in depth (Figures 8 and 9).

In a practical application, sources of environmental noise other than depth variation will be present and may also be limiting, for example atmospheric effects, which we neglect here. Our results indicate that it may be necessary to re-evaluate conclusions from previous studies that only consider differences between benthic types at specific uniform water depths without possibility of across-depth confusion [9].

Figure 8. Specific-depth results for separability of Bleached Coral, Dead Coral and Macroalgae from Live Coral for pure cover proportions (left column) and for 0.2 proportion (20%) in Live Coral (right column). Results are for specific uniform depths 0.5 m, 5 m, 20 m, and all IOP classes. Wind speed is 2 ms^{-1}, dotted and solid lines show sensor SNR 400:1 and 800:1. Error bars are ±1S.E across the ten repeat runs.

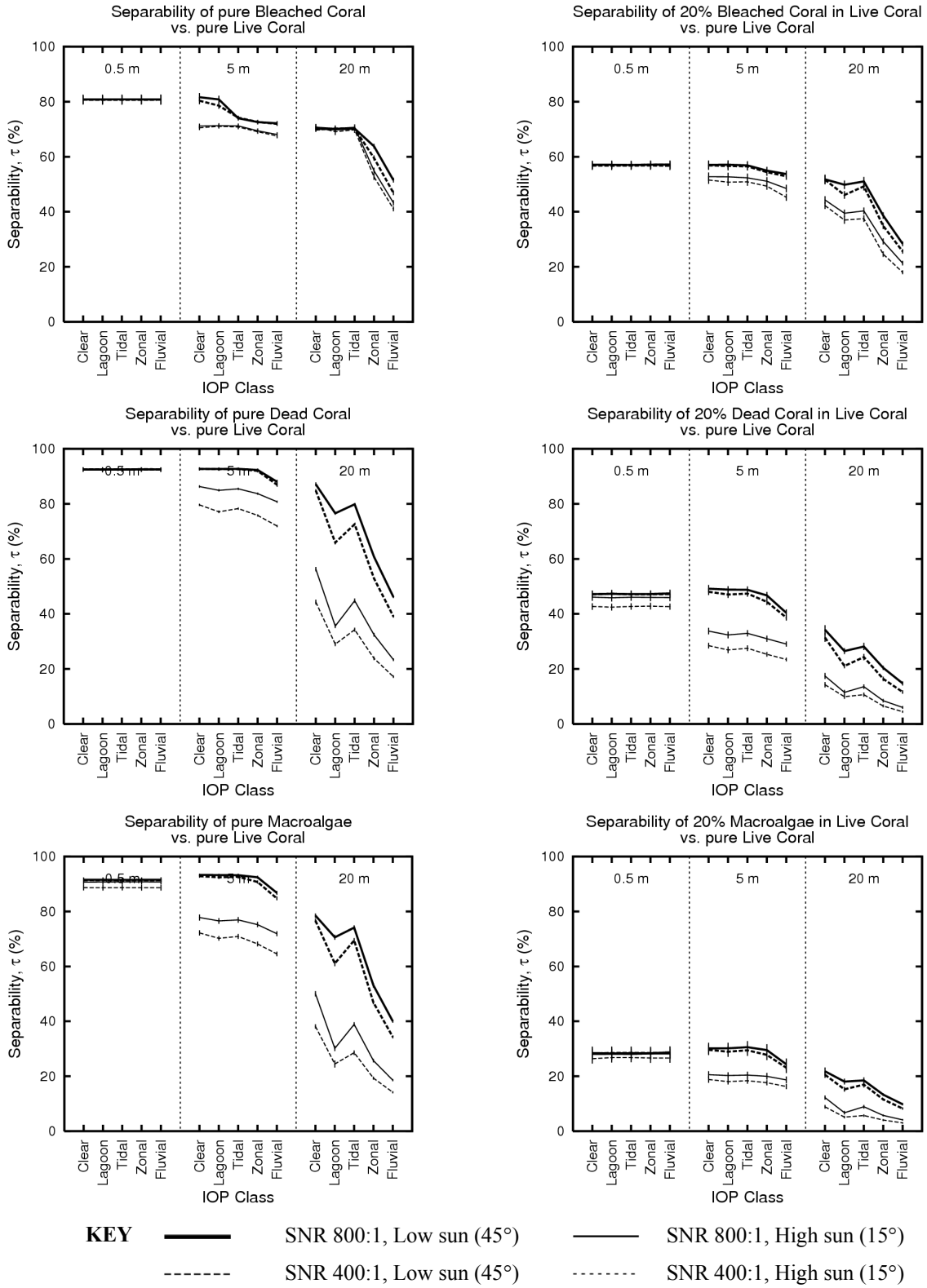

Figure 9. Depth-variable results for separability of Bleached Coral, Dead Coral and Macroalgae from Live Coral for pure cover proportions (left column) and for 0.2 proportion (20%) in Live Coral (right column). Results are for depth variation scenarios Shallow (0.5, 2 m), Shallow-Mid (0.5, 2, 5 m) and Shallow-Deep (0.5, 2, 5, 10, 20 m) combined with all IOP classes. Wind speed is 2 ms^{-1}, dotted and solid lines show sensor SNR 400:1 and 800:1. Error bars are ±1S.E across the ten repeat runs.

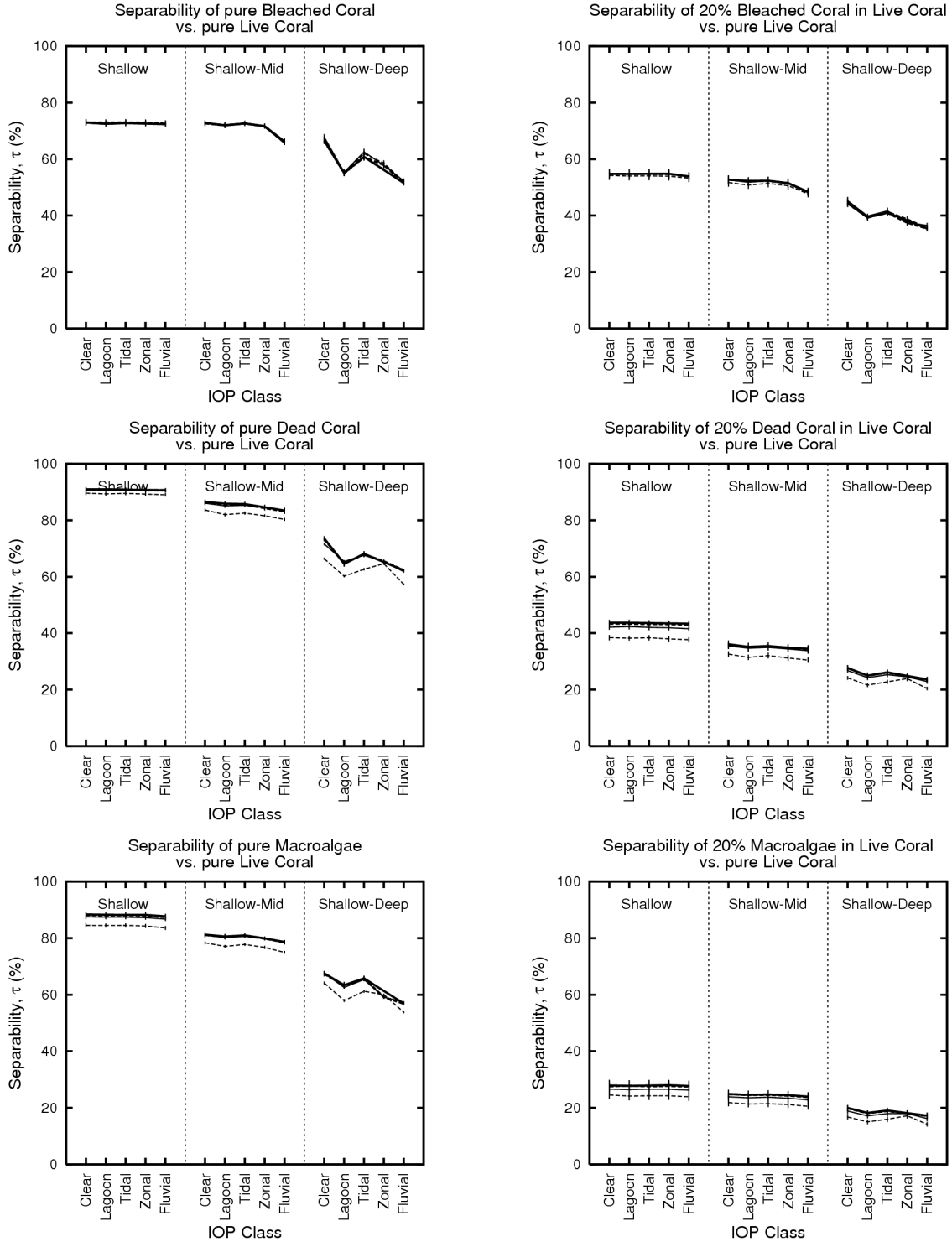

Finally, by way of a comparison to field-based data, we consider a published Pacific study [3] that demonstrated an improved ability to discriminate live from dead coral in approximate depth ranges of 2–3 m *vs.* 3–4 m in a 0.25 m pixel CASI image (SNR ~400:1) collected with solar zenith angle ~50°. In contrast, the modelling results here indicate no difference in separability for these classes in clear or lagoonal waters at specific depths of 0.5 m and 5 m for sun zenith 45° but a clear significant difference for sun zenith 15° or waters of lower clarity (Figure 8, centre left). However, the imagery in the published study [3] had only 6 spectral bands so our relative over-prediction of separability in the deeper waters may be due to the higher 15-band spectral resolution in the model. Extending the model framework to incorporate different spectral sensor configurations will answer this question and is a priority for future work.

3.4. Effect of Variation in IOP Values vs. *Absolute IOP Values*

Analogous to the previous discussion on depth, a distinction can be drawn between the effects of absolute water clarity on benthic class separability as opposed to the effects of variance in optical properties within an image. While neither absolute water clarity nor variance in clarity had much effect on benthic class separabilities in very shallow waters (0.5 m) absolute clarity within the modelled range starts to become limiting beyond 5 m while Zonal and Fluvial levels of variance have some effect at depths below 0.5 m (Table 4, Figure 8). Therefore, absolute water clarity and Tidal or Zonal IOP variation in the absence of terrestrial inputs and at moderate depths (<5 m) seems not to be a major confounding factor for benthic class separability. Since these conditions correspond to those found for much of coral reef remote sensing objectives then suitable analysis algorithms should be able to factor out water column effects [16,18,20,45]. Interpreting the total water column optical effect in terms of optical depth (optical depth = depth × attenuation), then it is clear that variation in depth will be more significant optically than the IOP variation in our dataset. Ratios between optical depths among the three physical depths 0.5, 5 and 20 m are 4, 10 and 40. Whereas relative attenuation between the IOP datasets has a maximum ratio of only around 10, or around 5 if the Fluvial class IOP datasets are excluded (Figure 5). If the ratio of 5, between minimum and maximum attenuations in the Lagoon class, is assumed as the typical range for reef remote sensing, then variation in IOPs will only become more optically significant than variation in depth if the depth range is restricted such that $d_{max}/d_{min} < 5$, for example, a depth range of 1 to 5 m or 2 to 10 m.

Discrimination of pure Bleached Coral from pure Live Coral presents an exception to the previous observation that Tidal variation IOPs overall had little effect (Figure 8, top left). While no significant difference exists in Bleached Coral separability under the single-dataset Clear or Lagoon classes, $\bar{\tau} = 81\%$ in both cases, Tidal IOP variation significantly reduces separability of Bleached Coral from Live Coral to $\bar{\tau} = 74\%$ ($p < 0.001$). This pattern occurs at both wind speeds (2 ms^{-1} and 8 ms^{-1}) but only for the high 800:1 SNR class and not when discriminating mixed proportions of Bleached Coral in Live Coral less than 1.0 (Figure 8, top right). In most cases sediments in coral reef environments will be dominated by calcium carbonate particles, and this was certainly true in our study sites where coral sand was abundant. Since detection of coral bleaching by remote sensing is essentially detecting a calcium carbonate "signal", *i.e.*, the coral skeleton with pigments removed, it is possible that variation in suspended sediments may be a confounding factor specifically for the detection of

bleaching. Our results support this hypothesis; in particular Figure 10 also indicates that variation in depth in Lagoon waters is a particular confounding factor for detecting Bleached Coral and also for Dead Coral, but less so Macroalgae. With respect to total water column backscatter, variation in depth under constant sediment load will to some extent act analogously to variation in sediment load. Therefore, both tidal depth in the presence of suspended sediments and changes in suspended sediment load may complicate detection of bleaching by optical remote sensing.

Figure 10. Separability of Bleached Coral, Dead Coral and Macroalgae from pure Live Coral under the three sensor noise classes and Zonal IOP variation as a function of depth. Error bars are ±1S.E over the ten repeat runs.

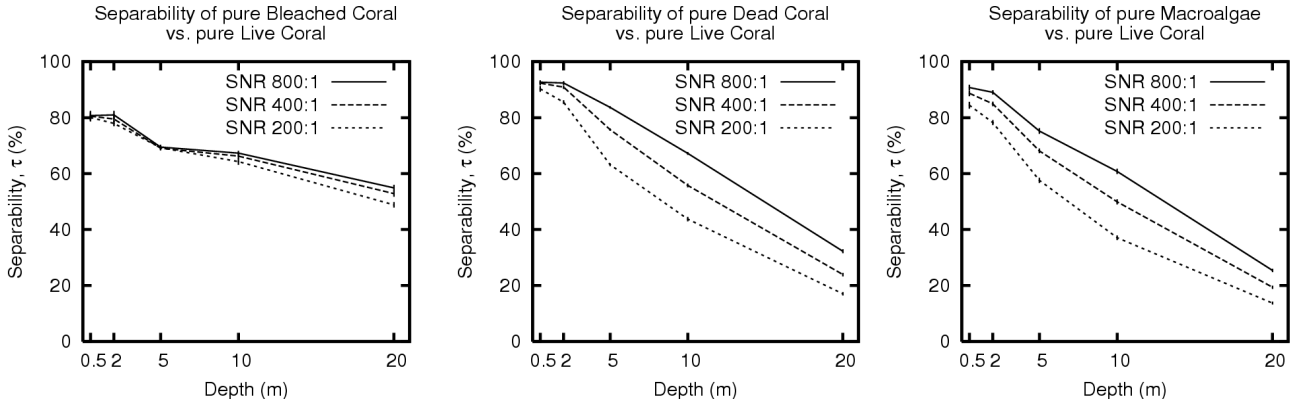

3.5. Sensor-Noise Limited vs. *Environmentally Limited Scenarios*

The vast majority of benthic class discrimination scenarios considered in the sensitivity analysis were not sensor-noise limited in the range of sensor SNR of 200:1 to 800:1. Of all 1440 class combination scenarios produced for both SNR 200:1 and SNR 400:1 only in 194 cases was there an increase in benthic class separability of five percentage points or more for the SNR 400:1 result, *i.e.*, 13% of the results were sensor-noise limited at the SNR 200:1 *vs.* 400:1 level. A threshold change in $\bar{\tau}$, $\Delta\bar{\tau} \geq 5\%$ was chosen to define a practical "limited" scenario rather than evaluating statistical significance of differences in $\bar{\tau}$, since $\bar{\tau}$ values can be statistically different by very small irrelevant amounts. By this criteria, the benefit of SNR 800:1 *vs.* 400:1 was even less significant, with 88 of 1,440 scenarios giving an SNR choice separability increase $\bar{\tau} > 5\%$., *i.e.*, only 6% of scenarios were sensor-noise limited.

Fundamental benthic class in situ spectral variation could be considered part of the "environment" and is always to some extent limiting since 100% separabilities were not achieved even with in situ reflectances (Figure 7). However, since here we are primarily concerned with the water column effects we consider "environmentally limited" scenarios to be those that were not limited by sensor SNR but for which separability was nevertheless reduced below the in situ maxima with $\Delta\bar{\tau} \geq 5\%$. By this criteria, 90% of scenarios were subject to separability limitation and removing the sensor-noise limited scenarios from this set leaves around 80% of scenarios as environmentally limited by factors other than basic *in situ* class overlap.

Table 5. Distribution of sensor limited scenarios in the sensitivity analysis as a function of benthic type to be discriminated from Live Coral, proportion of that type in Live Coral, sun zenith angle, wind speed and depth class: S = single-depth classes: 0.5 m, 5 m, 20 m; M = multiple-depth classes: Shallow, Shallow-Mid, Shallow-Deep. Each row represents *n* class combinations from the analysis and rows are hierarchically structured to focus on class combinations where sensor limitation occurred. Sensor limitation is presented as the percentage of class combination scenarios under which a doubling of sensor SNR produces in increase in benthic class separability, $\Delta\bar{\tau}$, of greater than five percentage points.

Benthic Type *vs.* Pure Live Coral.	**Mixture Proportion**	**Solar Zenith**	**Wind Speed**	**Depth Class**	***n***	**% of Sensor Limited Scenarios ($\Delta\bar{\tau} > 5\%$)**	
	%	**degrees**	**ms^{-1}**			**400:1 *vs.* 200:1**	**800:1 *vs.* 400:1**
Bleached Coral	any	any	any	any	480	1	0
Dead Coral	5%	any	any	any	120	0	0
	20%	45°	2	S	15	73	33
				M	15	53	0
			8	any	30	16	0
		15°	any	any	60	2	3
	50%	45°	2	S	15	73	53
				M	15	100	0
			8	any	30	37	33
		15°	any	any	60	17	13
	100%	45°	2	S	15	53	67
				M	15	67	13
			8	any	30	43	17
		15°	any	any	60	17	13
Macroalgae	5%	any	any	any	120	0	0
	20%	any	any	any	120	0	0
	50%	45°	2	S	15	67	33
				M	15	100	0
			8	any	30	20	10
		15°	any	any	60	13	3
	100%	45°	2	S	15	53	60
				M	15	100	0
			8	any	30	30	17
		15°	any	any	60	13	10

The distribution of scenarios that were sensor-noise limited in the sensitivity analysis was highly dependent on the environmental class combinations. For some specific environmental scenarios SNR limitation is significant (Table 4). In particular, for distinguishing Dead Coral or Macroalgae from Live Coral under sun elevation 45° and wind speed 2 ms^{-1}, doubling of SNR from 200:1 to 400:1 improved separability by greater than 5% for most depth and IOP classes. This implies that only under ideal environmental conditions of low sea surface reflection into upwelling radiance can sensor SNRs greater than 200:1 offer a significant advantage. Interestingly, under these circumstances, at the 200:1 *vs.* 400:1 SNR choice, almost all the multiple-depth classes were SNR limited whereas at the 400:1 to

800:1 choice none were (Table 4). This indicates the point at which depth variation overwhelmed sensor SNR as a confounding factor was around the SNR 400:1 level. Therefore, within the scope of this study, variation in depth was slightly less problematic for benthic class discrimination than the combination of sea surface state and sun elevation. Conversely, as discussed before, considering absolute depth as modelled by the single-depth classes, sensor-noise limitation continues to be predicted at the SNR 400:1 to 800:1 level under low sea surface reflection (Table 4). This again reiterates the point that considering separability only at specific uniform depths will over-emphasise the importance of sensor SNR.

Finally, note that discrimination of any mixture proportion of Bleached Coral from Live Coral was not sensor limited under almost any class combination scenario (Table 4). This is consistent with the earlier argument developed from the in situ results, that a large part of the Live Coral and Bleached Coral classes are highly separable, and hence do not require high sensor SNR to be discriminated. Unlike the Dead Coral and Macroalgae classes, the separability of Bleached Coral from Live Coral remains quite high as absolute depth increases and is relatively insensitive to sensor SNR (Figure 10). Therefore, different objectives within the scope coral reef remote sensing may demand different optimal sensor designs.

3.6. Hierarchical Analysis of Confounding Factors

Hierarchical summary diagrams (Figure 6) were constructed from the 1,440 factor combination scenarios to illustrate the relative significance of the various environmental and sensor class choices with respect to the entire sensitivity analysis for each basic benthic type (Figures 11–13). Each diagram should be read from top to bottom starting at the "All Scenarios" vertex, the vertical position of which indicates the mean separability over all 1,440 scenarios. Subsequent nodes indicate the mean separability as scenarios containing the most significant confounding factors are iteratively removed from the analysis (labelled arcs). At the bottom region of the graphs only the "ideal" scenarios for benthic class discrimination remain and the mean separability as represented by vertical position of the individual vertices is close to the maximum attainable under any scenario. The following sections discuss and interpret the patterns in these diagrams (Figures 11–13).

3.6.1. Initial Factor Exclusion—Sub-Pixel Proportions

Moving downwards from the "All Scenarios" node, in all three Figures 11–13 there is an initial large jump in overall accuracy attained by exclusion of all scenarios including the 0.05 benthic mixture proportion followed by the 0.2 and 0.5 cover proportions, although for Bleached Coral and Dead Coral exclusion of the 0.5 cover proportion class competes with 20 m depth and Deep multiple-depth class (Figures 11 and 12). This indicates that attempting to discriminate sub-pixel proportions of the benthic types was by far the biggest overall confounding factor for accuracy across the entire analysis. Any level of sub-pixel mixing, reduced overall separability to below 73%, and even to below 60% for Live Coral *vs.* Macroalgae. These results imply that benthic types that are mixed at sub-pixel scales will be subject to a potential error in cover estimate of around one third (*i.e.*, ~30%) of the areal extent of the type to be detected. This potential error rises to one half (~50%) for benthic types in sub-pixel proportions less than 0.2. This level of error is an upper limit and for some applications these

accuracies may be acceptable, but clearly subtle change detection or detection of partial bleaching events may be seriously confounded.

Figure 11. Hierarchical factor diagrams for separability of Bleached Coral from Live Coral. The diagram should be read vertically only, starting at the vertex labelled "All Scenarios". Subsequent arcs indicate the exclusion of classes as labelled (Table 2) with the vertical position of vertices showing mean separability over the remaining subset of scenarios. Vertices are spaced horizontally for clarity and horizontal position has no meaning. Lines A and B indicate narrow points in the graph network which partitions the results into regions. These regions represent groups of classes that have a similar effect on overall separability, with the most significant groups at the top of the figure. The region above line A separates sub-pixel mixtures and deep waters as the most important factors. Line B separates mid-depth waters from sensor noise, wind speed and sun elevation.

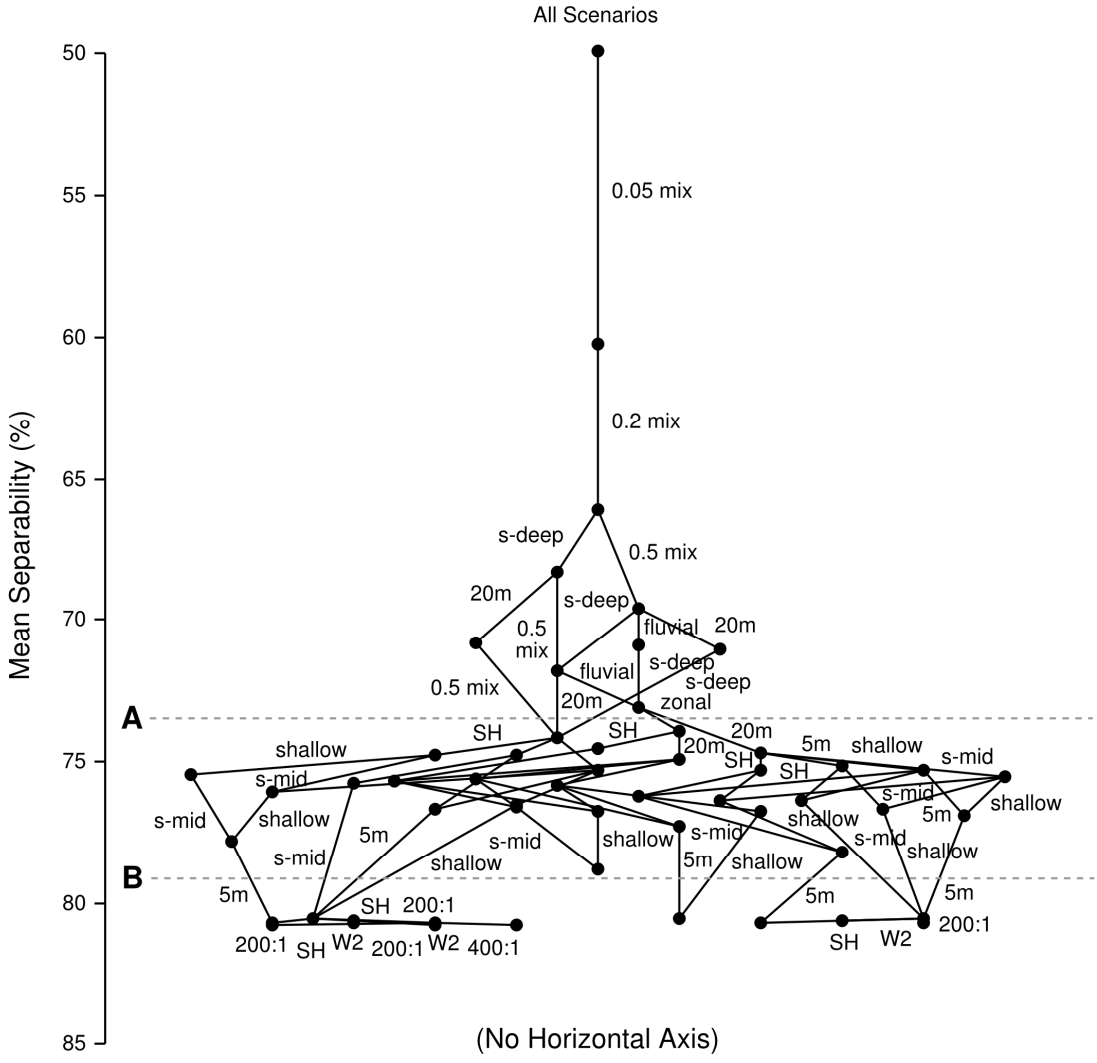

A previous study [3] using CASI imagery at with pixel resolutions of 1 m and 0.25 m pixels of a Pacific reef found no significant difference in classification accuracies of live and dead coral between the two resolutions, although the 0.25 m pixels would be expected to contain less sub-pixel benthic mixtures and hence give greater accuracy. The anomaly was explained by an estimated two-fold

increased environmental noise level in the higher resolution imagery, but in the results presented here an SNR increase did not compensate for any level of sub-pixel mixing. However, firstly, the interaction of benthic spatial distributions and pixel size was not assessed in [3], so it may not be true that the 0.25 pixels were less mixed. Secondly, the higher resolution imagery had a lower spectral resolution, 6 bands at 0.25 m *vs.* 10 bands at 1 m, and thirdly, the model presented here has a far higher diversity of coral reflectance (Table 2) whereas the area surveyed in [3] was dominated by only two genera (*Porites* and *Pocillopora*). These multiple qualifying factors illustrate the difficulty of making general inferences from image-based studies.

Figure 12. Hierarchical factor diagram for separability of Dead Coral from Live Coral. See caption of Figure 11 for full explanation.

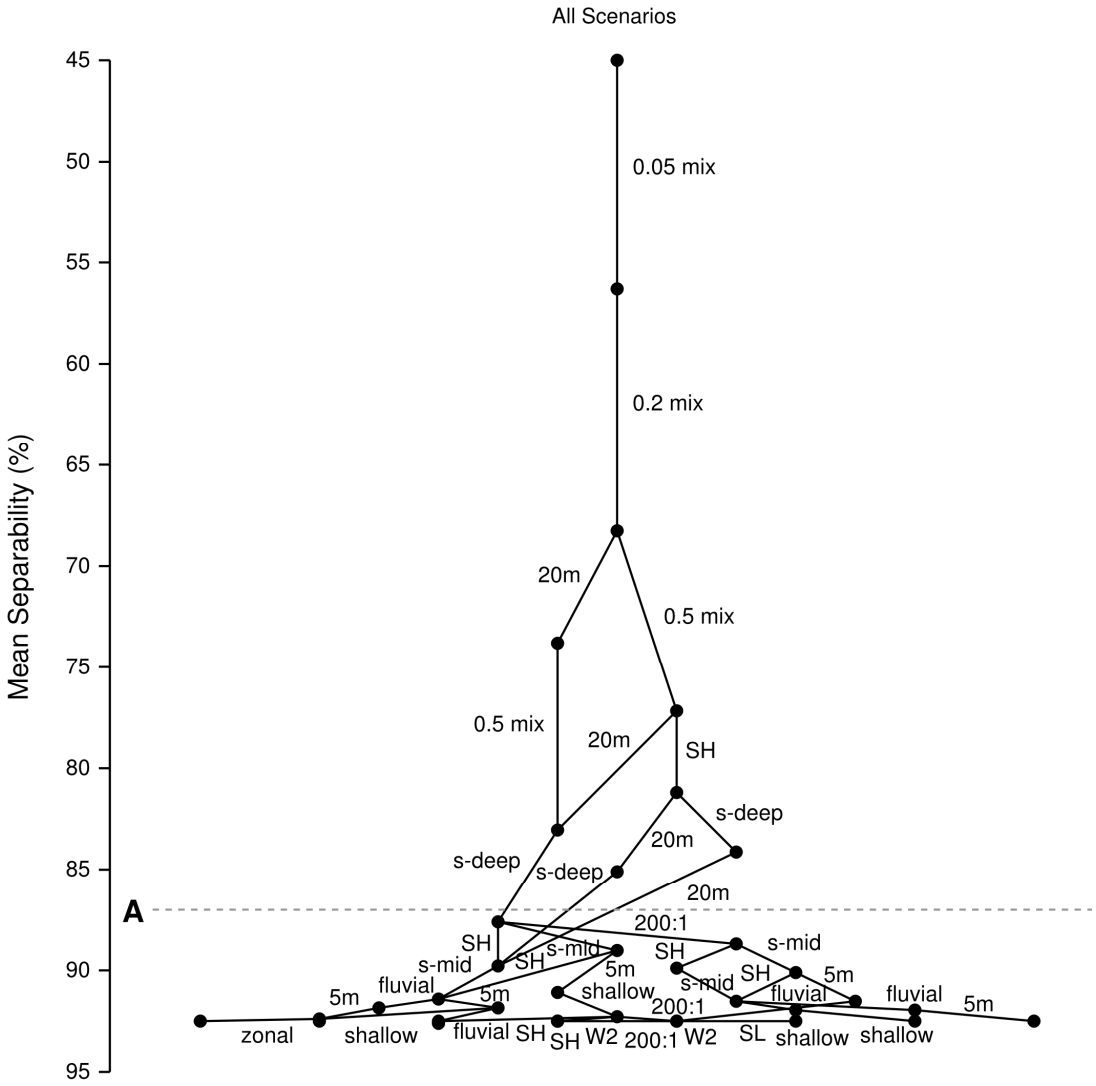

3.6.2. Second Tier—Water Depth and Sun Position

After the initial exclusion of sub-pixel mixtures, all three diagrams of Figures 11–13 exhibit a widening due to multiple possibilities for subsequent class exclusions followed by a narrowing representing convergence on a specific set of class exclusions (line A in Figures 11–13). In each diagram, this group of classes represents a second tier of accuracy confounding factors that operated

after sub-pixel proportions had been excluded. A water depth of greater than 5 m was the most significant confounding factor across all three graphs at this stage with almost all scenarios containing the 20 m and the Shallow-Deep classes removed from the analysis by this point. Additionally, differences among the benthic types start to emerge with many exclusions of high sun elevation for Dead Coral and Macroalgae *vs.* the exclusion of the Fluvial IOP class from a large subsection of the Bleached Coral diagram. Overall therefore, deep water was the next most significant confounding factor for benthic class discrimination after sub-pixel proportions, followed by high sun position. Reasonable water clarity was also important for detecting bleached coral at this accuracy level.

Figure 13. Hierarchical factor diagram for separability of Macroalgae from Live Coral. See caption of Figure 11 for full explanation.

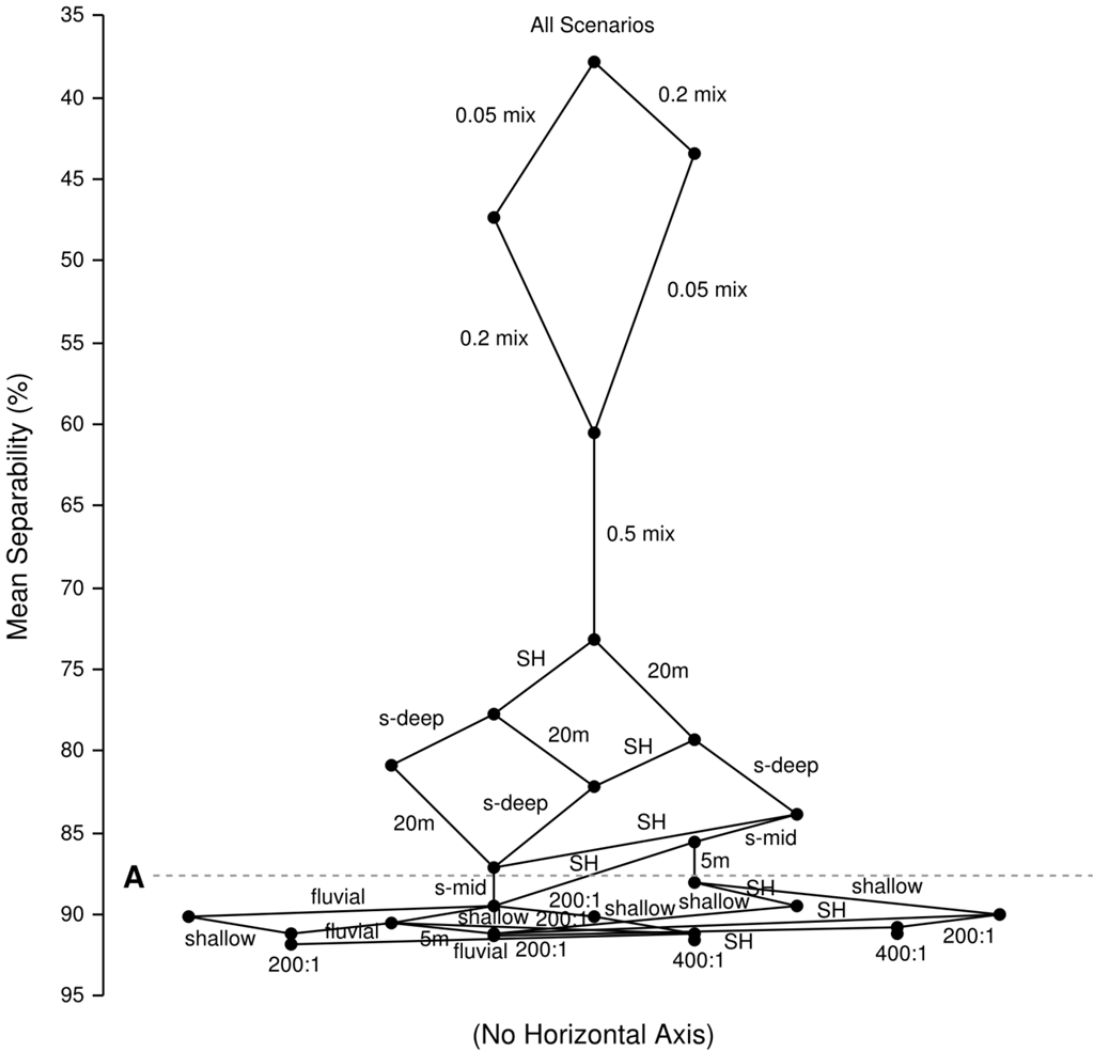

3.6.3. High Accuracy Plateau—Insignificant Factors

The final section common to all three class significance graphs is a high accuracy plateau, where elimination of the main confounding factors increased mean separability to a value within an few percent of the maximum attainable. At this stage there are many options for exclusion of the remaining classes since all only had a small effect on overall accuracy. Visually this is apparent by the widening of the graph diagrams out to a flat base (Figures 11–13). Classes that appear within this plateau were of

very little relative significance within the sensitivity analysis as a whole. For all three benthic types excluded factors at this stage typically included the sensor SNR classes, wind speed classes and almost all IOP classes, for clarity Figures 11–13 do not include all of these arcs and vertices. The Bleached Coral graph is notable in that there is a clear intermediate step to high accuracy where remaining depth classes except 0.5 m were excluded (line B in Figure 11). This indicates that any water depth greater than 0.5 m was a confounding factor for detecting bleaching. The same effect is present but less pronounced for Dead Coral and Macroalgae (Figures 12 and 13).

In the Bleached Coral diagram (Figure 11) there is a division into two subsections where in one case the Fluvial IOP class was excluded and in the other it was retained. The division occurs at the point where line A intersects the graph and persists to the high separability plateau, where the group of four vertices on the left still contains the Fluvial IOP class but the three on the right do not. This illustrates the interaction between water clarity and depth, as large depths were excluded low water clarity became increasingly insignificant. Note however that the trade-off is highly unbalanced since the graph construction implies that at almost every step excluding a depth class is twice as effective as excluding an IOP class. This is consistent with the charts in Figures 8 and 9, which illustrate IOP class only had a large effect on separability in the 20 m and Shallow-Deep classes.

The overall structure of the hierarchical graphs and subsequent conclusions are dependent on the design of the sensitivity analysis class structure and the methodology of graph construction. However, the class structure was designed to represent scenarios encountered in practical reef remote sensing contexts. The major patterns in the results are fairly clear and consistent between the detailed analysis (Figures 8 and 9) and the hierarchical summary (Figures 11–13) and can be further qualitatively summarised as a single ranked list of confounding factors for benthic remote sensing, Table 6.

Table 6. Overall list of confounding factors for accuracy of benthic type separability ordered by significance (based on the structure of the experiment design presented here).

(1) Detecting proportions less than 100% of any benthic type.
(2) Water depth > 5m.
(3) Fluvial variation in IOPs when detecting bleaching.
(4) High sun elevation (zenith angle 15° *vs.* 45°).
(5) Water depth > 0.5 m when detecting bleaching (less important for dead coral or macroalgae).
(6) Sensor SNR, wind speed and other IOP variations are overall not very significant factors.

4. Conclusions

One of the aims of this study has been to demonstrate a generic method for analysing a remote sensing system in terms of individual environmental and sensor components. The aim of this method is to be able to distinguish between environmentally limited objectives, where accuracy cannot benefit from improved sensor design, and sensor-limited objectives, where specific sensor design improvements will be effective and their effect on accuracy can be quantitatively predicted. Although this paper has concentrated on benthic class separability, it is straightforward to turn the analysis around and instead, for example, consider the capability to recover bathymetry or IOP class under benthic class variation.

Within the scope of the experimental design presented here, the relative importance of several key environmental and sensor design factors in accurately discriminating benthic classes in remotely sensed image data has been established. For the benthic types considered here, sub-pixel quantification was the most challenging objective. While previous modelling studies have not quantified the effect of benthic class confusion across depths, this work has demonstrated that while depth itself is a serious confounding factor for benthic remote sensing, depth variation introduces further spectral confusion even for shallow waters (<2 m). *That is*, the fact that we do not know a priori exactly what depth a pixel represents is a separate source of confusion than the fact that increasing depth attenuates the reflected light. Overall, water column IOP spatial variation found in reef systems does little to confound benthic class separability. This result supports the application of the latest techniques that aim to extract both water properties and benthic class from optical data [19]. While most environmental factors cannot be controlled by investigators, our model framework provides a method for determining optimal conditions for those that can. This is demonstrated by the highlighting of sun elevation at image acquisition as an important factor in the hierarchy of confounding factors (Table 6). An efficient software implementation of the method could therefore be a useful planning tool for remote sensing campaigns.

Overall, most modelled scenarios were environmentally limited, with sensor SNR limitation only becoming significant under ideal environmental conditions of low wind speed and low sun elevation and for certain benthic classes. However, sub-pixel mixing can be interpreted indirectly as a sensor characteristic through being a function of spatial resolution. Since sub-pixel mixing was an overwhelming confounding factor in the analysis and sensor SNR was not, it may be that current airborne sensors would benefit in trading SNR for higher spatial resolution in reef applications. Identifying the optimal spatial resolution will require an analysis of benthic spatial distributions on reefs, but even a qualitative assessment based on experience of the scales of heterogeneity in reef environments implies that in general resolutions below 1 m^2 are required. Importantly, if future predictions of decline of live coral cover on reefs are borne out, the difficulty in monitoring these ecosystems by remote sensing will only increase. While bleached coral was the most robustly discriminated benthic class under the range of conditions modelled, since bleaching events occur on relatively short time scales of days to weeks the practical advantage of this detectability may outweighed by the temporal resolution offered by satellite over-flight times, or the need to plan airborne surveys.

For high spatial resolutions, water column effects causing lateral spectral mixing must also be considered, *i.e.*, the water column "point spread function" [24], plus effects due to benthic 3-dimensional canopy structure. These effects cannot be assessed with the plane-parallel radiative transfer model used here and so will require new modelling algorithms [31]. For satellite-borne sensors atmospheric effects will also be a significant factor that will affect the balance of sensor SNR and spatial resolution. In this study we have neglected to consider differing sensor spectral resolutions as this has been addressed before [6,7]. However this design factor will also be trade-off with SNR and spatial resolution and cannot be treated in isolation from these or the environmental factors included here. Future work will extend the model framework presented here to incorporate all the above-discussed factors, the primary difficulty being to make the resulting multi-factor analysis computationally tractable. Nevertheless,

developing such a generic modelling framework would seem a highly cost-effective method for improving understanding of remote sensing systems and advising on future practical directions.

With respect to the estimated separabilities presented here, as the current model is simplified in certain respects and excludes an atmospheric component, these will be upper bounds on what will be achievable in practice. Although it could be argued that non-linear analysis techniques such as successive approximation models, look-up tables or neural networks [17,18,46,47] may perform better under certain circumstances than the linear separability measure used here, the significant spectral space class overlap that must be present for some factor combinations will confound any analytical method. Similarly, any pre-processing steps that only manipulate individual pixel spectra, such as removing water column effects by depth invariant indices [22,44] will have little impact on separability as identical spectra remain identical after transformation. Conversely, techniques that incorporate additional data sources such a sonar bathymetry [48], do in theory add information and could resolve cases of spectral confusion. Therefore, while there are definite environmental limitations to what can be achieved by any sensor or algorithm, the future potential to overcome these limitations resides in data synthesis across multiple sources.

Acknowledgements

This project was funded by the World Bank/GEF Coral Reef Targeted Research and Capacity Building Program with additional contributions from the UK Natural Environment Research Council (grants NER/Z/S/2001/01029 and NE/C513626/1) and the Australian Research Council Discovery Project (DP0663893. Innovative Coral Reef Mapping) to Phinn and Mumby. The authors are grateful for the assistance of the University of the South Pacific and the South Pacific Geosciences Committee. The manuscript was improved thanks to the comments of Edward Smith.

References

1. Elvidge, C.D.; Dietz, J.B.; Berklemans, R.; Andréfouët, S.; Skirving, W.; Strong, A.E.; Tuttle, B.T.; Satellite observation of Keppel Islands (Great Barrier Reef) 2002 coral bleaching using IKONOS data. *Coral Reefs* **2004**, *23*, 123-132.
2. Mumby, P.J.; Chisholm, J.R.M.; Clark, C.D.; Hedley, J.D.; Jaubert, J. A bird's eye view of the health of coral reefs. *Nature* **2001**, *413*, 36.
3. Mumby, P.J.; Hedley, J.D.; Chisholm, J.R.M.; Clark, C.D.; Ripley, H.; Jaubert, J. The cover of living and dead corals from airborne remote sensing. *Coral Reefs* **2004**, *23*, 171-183.
4. Hedley, J.D.; Mumby, P.J. Biological and remote sensing perspectives of pigmentation in coral reef organisms. *Adv. Mar. Biol.* **2002**, *43*, 277-317.
5. Lesser, M.P.; Mobley, C.D. Bathymetry, water optical properties, and benthic classification of coral reefs using hyperspectral remote sensing imagery. *Coral Reefs* **2007**, *26*, 819-829.
6. Hochberg, E.J.; Atkinson, M.J.; Andréfouët, S. Spectral reflectance of coral reef bottom types worldwide and implications for coral reef remote sensing. *Remote Sens. Environ.* **2003**, *85*, 159-173.
7. Hochberg, E.J.; Atkinson, M.J. Capabilities of remote sensors to classify coral, algae and sand as pure and mixed spectra. *Remote Sens. Environ.* **2003**, *85*, 174-189.

8. Karpouzli, E.; Malthus, T.J.; Place, C.J. Hyperspectral discrimination of coral reef benthic communities in the western Caribbean. *Coral Reefs* **2004**, *23*, 141-151.
9. Kutser, T.; Dekker, A.G.; Skirving, W. Modeling spectral discrimination of Great Barrier Reef benthic communities by remote sensing instruments. *Limnol. Oceanogr.* **2003**, *48*, 497-510.
10. Lubin, D.; Li, W.; Dustan, P.; Mazel, C.H.; Stamnes, K. Spectral Signatures of coral reefs: Features from space. *Remote Sens. Environ.* **2001**, *75*, 127-137.
11. Malthus, T.; Mumby, P.J. Remote sensing of the coastal zone: An overview and priorities for future research. *Int. J. Remote Sens.* **2003**, *24*, 2805-2815.
12. Phinn, S.R.; Dekker, A.G.; Brando, V.E.; Roelfsema, C.M. Mapping water quality and substrate cover in optically complex coastal and reef waters: An integrated approach. *Mar. Pollut. Bull.* **2005**, *51*, 459-469.
13. Hedley, J.D.; Mumby, P.J.; Joyce, K.E.; Phinn, S.R. Spectral unmixing of coral reef benthos under ideal conditions. *Coral Reefs* **2004**, *23*, 60-73.
14. Hedley, J.D.; Mumby, P.J. A remote sensing method for resolving depth and subpixel composition of aquatic benthos. *Limnol. Oceanogr.* **2003**, *48*, 480-488.
15. Lee, Z.P.; Carder, K.L.; Mobley, C.D.; Steward, R.G.; Patch, J.S. Hyperspectral remote sensing for shallow waters, 1. A semi-analytical model. *Appl. Opt.* **1998**, *37*, 6329-6338.
16. Lee, Z.P.; Carder, K.L.; Mobley, C.D.; Steward, R.G.; Patch, J.S. Hyperspectral remote sensing for shallow waters, 2. Deriving bottom depths and water properties by optimization. *Appl. Opt.* **1999**, *38*, 3831-3843.
17. Lee, Z.; Carder, K.L.; Chen, R.F.; Peacock, T.G. Properties of the water column and bottom derived from Airborne Visible Infrared Imaging Spectrometer (AVIRIS) data. *J. Geophys. Res.* **2001**, *106*, 11639-11651.
18. Mobley, C.D.; Sundman, L.K.; Davis, C.O.; Bowles, J.H.; Downes, T.V.; Leathers, R.A.; Montes, M.J.; Bisset, W.P.; Kohler, D.D.R.; Reid, R.P.; Louchard, A.M.; Gleason, A. Interpretation of hyperspectral remote-sensing imagery by spectrum matching and look-up tables. *Appl. Opt.* **2005**, *44*, 3576-3592.
19. Brando, V.E.; Anstee, J.M.; Wettle, M.; Dekker, A.G.; Phinn, S.R.; Roelfsema, C. A physics based retrieval and quality assessment of bathymetry from suboptimal hyperspectral data. *Remote Sens. Environ.* **2009**, *113*, 755-770.
20. Hedley, J.D.; Roelfsema, C.M.; Phinn, S.R. Efficient radiative transfer model inversion for remote sensing applications. *Remote Sens. Environ*. **2009**, *113*, 2527-2532.
21. Dekker, A.G.; Phinn, S.R.; Anstee J.; Bissett P.; Brando V.E.; Casey B.; Fearns P.; Hedley, J.; Klonowski W.; Lee, Z.P.; Lynch, M.; Lyons, M.; Mobley, C.; Roelfsema, C. Intercomparison of shallow water bathymetry, hydro-optics, and benthos mapping techniques in Australian and Caribbean coastal environments. *Limnol. Oceanogr. Methods* **2011**, *9*, 396-425.
22. Green, E.P.; Mumby, P.J.; Edwards A.J.; Clark, C.D. *Remote Sensing Handbook for Tropical Coastal Management*; UNESCO: Paris, France, 2000.
23. Mobley, C.D. Thematic mapping. In *Ocean Optics Web Book*; 2012. Available online: http://www.oceanopticsbook.info/view/remote_sensing/level_2/thematic_mapping (accessed on 20 January 2012).

24. Mobley, C.D.; Sundman, L.K. Effects of optically shallow waters on upwelling radiances: Inhomogeneous and sloping bottoms. *Limnol. Oceanogr.* **2003**, *48*, 329-336.
25. Grant, R.H.; Hiesler, G.M.; Gao, W. Photosynthetically-active radiation: Sky radiance distributions under clear and overcast conditions. *Agric. For. Meteorol.* **1996**, *82*, 267-292.
26. Cox, C.; Munk, W. Statistics of the sea surface derived from sun glitter. *J. Mar. Res.* **1954**, *13*, 198-227.
27. Mobley, C.D. *Light and Water*; Academic Press: San Diego, CA, USA, 1994.
28. Mather, P.M. *Computer Processing of Remotely-Sensed Images*, 2nd ed.; Wiley: New York, NY, USA, 1999.
29. Lucas, R.; Rowlands, A.; Niemann, O.; Merton, R.N. Hyperspectral sensors and applications. In *Advanced Image Processing Techniques for Remote Sensed Hyperspectral Data*; Varshney, P.K., Arora, M.J., Eds.; Springer-Verlag: New York, NY, USA, 2004; pp. 11-49.
30. Roelfsema, C.M.; Marshall, J.; Hochberg, E.; Phinn, S.; Goldizen, A.; Joyce, K. *Underwater Spectrometer System 2004 (UWSS04)*; Centre for Remote Sensing and Spatial Information Science, University of Queensland: Brisbane, QLD, Australia, 2006.
31. Hedley, J. A three-dimensional radiative transfer model for shallow water environments. *Opt. Express* **2008**, *16*, 21887-21902.
32. Mobley, C.D.; Sundman, L.K. *Hydrolight 4.1 Users' Guide*; Sequoia Scientific Inc.: Redmond, WA, USA, 2000.
33. Hedley, J.D.; Harborne, A.R.; Mumby, P.J. Simple and robust removal of sun glint for mapping shallow water benthos. *Int. J. Remote Sens.* **2005**, *26*, 2107-2112.
34. Mueller, J.L. *Ocean Optics Protocols for Satellite Ocean Color Sensor Validation*; NASA/TM 2003-211621/Rev 4-Vol IV (Erratum 1); 2003.
35. Smith, R.C.; Baker, K.S. Optical properties of the clearest natural waters (200–800 nm). *Appl. Opt.* **2001**, *20*, 177-184.
36. Boss, E.; Pegau, W.S. Relationship of light scattering at an angle in the backward direction to the backscattering coefficient. *Appl. Opt.* **2001**, *40*, 5503-5507.
37. Mobley, C.D.; Sundman, L.K.; Boss, E. Phase function effects on oceanic light fields. *Appl. Opt.* **2002**, *41*, 1035-1050.
38. Karpouzli, E.; Malthus, T.; Place, C.; Mitchell Chui, A.; Ines Garcia, M.; Mair, J. Underwater light characterisation for correction of remotely sensed images. *Int. J. Remote Sens*. **2003**, *24*, 2683-2702.
39. Tabachnick, B.G.; Fidell, L.S. *Using Multivariate Statistics*, 4th ed.; Allyn and Bacon: London, UK, 2001.
40. Ma, Z.; Redmond, R.L. Tau coefficients for accuracy assessment of classification of remotely sensed data. *Photogramm. Eng. Remote Sensing* **1995**, *61*, 435-439.
41. Sokal, R.R.; Rohlf, F.J. *Biometry*, 3rd ed.; Freeman: San Francisco, CA, USA, 1995.
42. Christofides, N. *Graph theory. An algorithmic approach.* Academic Press, London, UK, 1975.
43. Leiper, I.A.; Siebeck, U.E.; Marshall, N.J.; Phinn, S.R. Coral health monitoring: Linking coral colour and remote sensing techniques. *Can. J. Remote Sensing* **2009**, *35*, 276-286.
44. Lyzenga, D.R. Passive remote sensing techniques for mapping water depth and bottom features. *Appl. Opt.* **1978**, *17*, 379-383.

45. Wettle, M.; Brando, V.E. *SAMBUCA: Semi-Analytical Model for Bathymetry, Un-Mixing, and Concentration Assessment*; CSIRO Land and Water Science Report 22/06; CSIRO: Canberra, ACT, Australia, 2006.
46. Calvo, S.; Ciraolo, G.; La Loggia, G. Monitoring Posidonia oceanica meadows in a Mediterranean coastal lagoon (Stagnone, Italy) by means of neural network and ISODATA classification methods. *Int. J. Remote Sens.* **2003**, *24*, 2703-2716.
47. Ceyhun, Ö.; Yalcin, A. Remote sensing of water depths in shallow waters via artificial neural networks. *Estuar. Coast. Shelf Sci.* **2010**, *89*, 89-96.
48. Bejerano, S.; Mumby, P.J.; Hedley, J.D.; Sotheran, I. Combining optical and acoustic data to enhance the detection of Caribbean fore-reef habitats. *Remote Sens. Environ.* **2010**, *114*, 2768-2778.